- 1 Atmospheric chemical processing dictates aerosol aluminum solubility: insights from
- 2 field measurement at two locations in northern China

- 4 Tianyu Zhang,^{1,5} Yizhu Chen,^{1,5} Huanhuan Zhang,² Lei Liu,³ Chengpeng Huang,⁴ Zhengyang
- 5 Fang,^{1,a} Yifan Zhang,^{1,5} Fu Wang,⁴ Lan Luo,⁴ Guohua Zhang,¹ Xinming Wang,¹ Mingjin
- 6 Tang^{1,6,*}

7

- 8 ¹ State Key Laboratory of Advanced Environmental Technology and Guangdong Key
- 9 Laboratory of Environmental Protection and Resources Utilization, Guangzhou Institute
- of Geochemistry, Chinese Academy of Sciences, Guangzhou, China
- ² Guangzhou Marine Geological Survey, China Geological Survey, Guangzhou, China
- 12 ³ Hangzhou International Innovation Institute, Beihang University, Hangzhou, China
- ⁴ Longhua Center for Disease Control and Prevention of Shenzhen, Shenzhen, China
- ⁵ College of Earth and Planetary Sciences, University of Chinese Academy of Sciences, Beijing,
- 15 China
- 16 ⁶ Institute of Surface-Earth System Science, School of Earth System Science, Tianjin
- 17 University, Tianjin, China
- ^a Current address: Institute of Low Temperature Science, Hokkaido University, Sapporo, 060-
- 19 0819, Japan
- 20 Correspondence: Mingjin Tang (mingjintang@126.com)

21

Abstract

23

24

25

26

27

28

29

30

31

32

33

34

35

36

37

38

39

40

41

Deposition of mineral dust aerosol into open oceans greatly impacts marine biogeochemistry and primary production, and the deposition rates can be constrained using dissolved aluminum (Al) in surface seawater as a tracer. However, aerosol Al solubility, a critical parameter used in this method, remains highly uncertain. This work investigated seasonal variations of aerosol Al solubility for supermicron and submicron particles at two locations (Xi'an and Qingdao) in northern China. Aerosol Al solubility was found to be very low at Xi'an and much higher at Qingdao. Furthermore, seasonal variability of Al solubility, its correlation with relative abundance of sulfate and nitrate, and its dependence on relative humidity, are all different at the two locations. We suggest that all the features observed for aerosol Al solubility at the two locations can be well explained by the effects of atmospheric chemical processing. Mineral dust transported to Xi'an (an inland city in Northwest China) was still not obviously aged and thus chemical processing had little effects on aerosol Al solubility. After arriving g at Qingdao (a coastal city in the Northwest Pacific), mineral dust was substantially aged by chemical processing, leading to substantial enhancement in aerosol Al solubility. Our work further reveals that aerosol liquid water and acidity play vital roles in the dissolution of aerosol Al by atmospheric chemical processing. We suggest that spatial variation of aerosol Al solubility should be taken into account so that oceanic dust deposition can be better constrained using dissolved Al concentrations in surface seawater.

43

1. Introduction

45

46

47

48

49

50

51

52

53

54

55

56

57

58

59

60

61

62

63

64

65

66

As an important type of tropospheric aerosols, mineral dust aerosol greatly impacts atmosphere chemistry, climate, and ecological systems (Jickells et al., 2005; Tang et al., 2016; Kok et al., 2023). After long-range transport, deposition of mineral dust into the oceans is a major external source of several nutrient and toxic elements for surface seawater (Moore et al., 2013; Westberry et al., 2023), impacting primary production and biogeochemical cycles in the oceans and having further feedback on the climate system (Mahowald, 2011; Jiang et al., 2024). The deposition flux of mineral dust aerosol into the oceans should be accurately estimated before we can assess its impacts on marine biogeochemistry in a reliable manner (Schulz et al., 2012; Anderson et al., 2016). Previous studies used several different methods to estimate dust deposition fluxes and found large discrepancies (Huneeus et al., 2011; Anderson et al., 2016). Deposition of mineral dust aerosol is the dominant source of dissolved aluminum (Al) in the surface water of open oceans, and dissolved Al is generally considered to be chemically and biologically inactive in seawater. As a result, dissolved Al concentrations in surface seawater could be used to calculate dust deposition flux into the oceans (Measures and Brown, 1996; Measures and Vink, 2000), and the fractional solubility of aerosol Al (the fraction of aerosol Al that can be dissolved) is one of the key parameters used in this method. Previous studies which used this method to estimate dust depositions fluxes (Han et al., 2008; Measures et al., 2010; Grand et al., 2015; Benaltabet et al., 2022) usually assumed uniform Al solubility values in the range of 1.5-5%. However, field measurements found that aerosol Al solubility could vary by more than an order of magnitude (Baker et al., 2006; Buck et al., 2013), and thereby using a uniform aerosol Al solubility value could lead to large uncertainties in

estimated dust deposition fluxes (Han et al., 2008; Xu and Weber, 2021). As a result, it is important to understand the spatiotemporal variations of aerosol Al solubility and elucidate the processes and mechanisms which drive such variations.

67

68

69

70

71

72

73

74

75

76

77

78

79

80

81

82

83

84

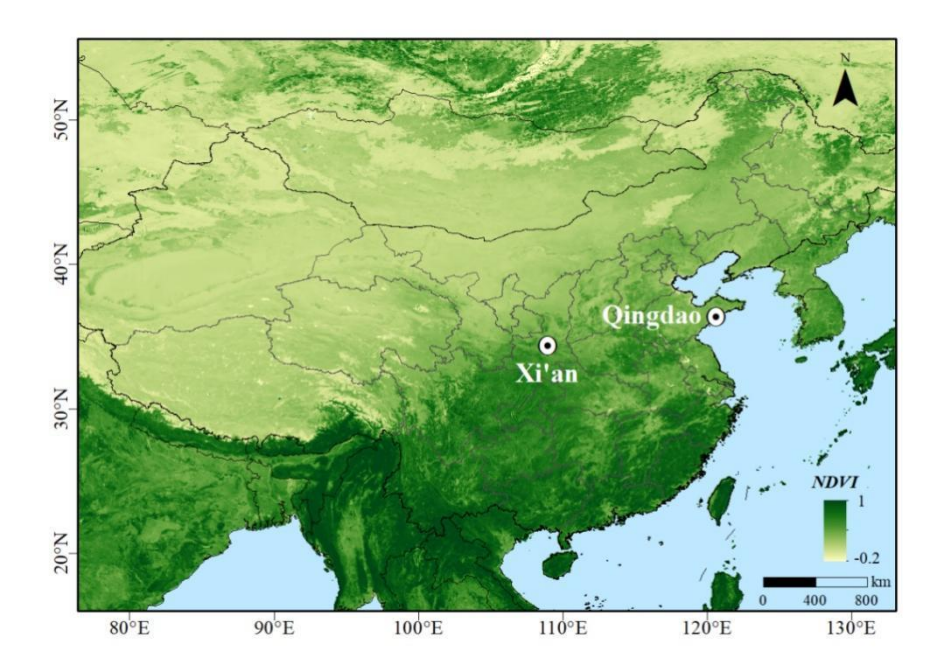
85

86

87

The initial Al solubility is generally low (typically <1.5%) for dust particles over desert regions (Shi et al., 2011; Aghnatios et al., 2014; Li et al., 2022), and field studies found that aerosol Al solubility in the troposphere could be much higher and showed wide variability. For example, Al solubility ranged from 0.2-15.9% for total suspended particles (TSP) over the Pacific (Buck et al., 2013), and were in the range of 3-78% over the Atlantic (Buck et al., 2010; Chance et al., 2015). Some studies (Measures et al., 2010; Sakata et al., 2023) found good correlations between dissolved aerosol Al (or Al solubility) and acid species in aerosol particles, and thus suggested that chemical processes in the atmosphere could substantially enhance aerosol Al solubility; furthermore, Li et al. (2017) found that Al solubility was remarkably increased during cloud events when cloud processing enhanced the formation of secondary inorganic ions (mainly sulfate and nitrate) and thus increased the acidity of cloud droplets. However, Yang et al. (2023) found no correlations between Al solubility and the concentrations of aerosol acidic species, and concluded that the effect of acid processing on Al solubility was negligible. Aerosol Al solubility over the Atlantic appeared to be higher for air masses from Europe than those from the Saharan region (Baker et al., 2006; López-García et al., 2017), and some studies hypothesized that this could be potentially explained by the influence of anthropogenic aerosol Al if it had higher solubility than mineral dust (Paris et al., 2010; López-García et al., 2017).

It can be concluded that although aerosol Al solubility in the atmosphere was explored by several previous studies, our understanding is still very limited. For example, it remains unclear why aerosol Al solubility shows large spatial and temporal variation. Some work suggested that atmospheric chemical aging could enhance aerosol Al solubility, but the mechanisms and key environmental factors have not been elucidated. Furthermore, the effects of particle size on aerosol Al solubility have not been well understood.



94

95

96

97

88

89

90

91

92

93

Figure 1. A map of East Asia and surrounding areas. The two locations (Xi'an and Qingdao) where we collected aerosol particles are highlighted. NDVI: normalized difference vegetation index provided by MODIS (Moderate Resolution Imaging Spectroradiometer).

98

99

100

101

102

In this work, we collected supermicron (>1 μm) and submicron (<1 μm) aerosol particles at Xi'an and Qingdao, both located in northern China, and investigated seasonal variations of aerosol Al solubility at these two locations. Taklimakan and Gobi Deserts in northwestern China are two important source regions of Asian dust (Prospero et al., 2002). As shown in Figure 1, Xi'an is an inland city in northwestern China, and the aging extent of dust was found to be quite limited at Xi'an due to its proximity of desert regions (Wang et al., 2014; Wu et al., 2017). As Asian dust is transported eastward, it passes over the North China Plain where anthropogenic emission is very high, and may become much more aged when arriving at Qingdao, a coastal city of the Northwest Pacific (Li et al., 2014; Pan et al., 2017). By comparing aerosol Al solubility at Xi'an and Qingdao, our work can provide valuable insights into how and to which extent aging processes during long-range transport can change aerosol Al solubility. Dust aerosol concentrations and meteorological conditions vary remarkably at different seasons in Northern China; as a result, examining its seasonal variations provides a good opportunity to understand the factors which regulate aerosol Al solubility.

2. Materials and methods

2.1 Sample collection

Samples were collected at two cities (Xi'an and Qingdao) in northern China at four different seasons during 2021-2023 (Zhang et al., 2023; Chen et al., 2024), and further details can be found in the supplement (Text S1 and Table S1). In brief, supermicron (>1 μm) and submicron (<1 μm) particles were simultaneously collected using a two-stage aerosol sampler (TH-150C, Tianhong Co., China) which was operated at 100 L/min, and the sampling duration was typically 23.5 hours for each pair of aerosol samples. Whatman 41 cellulose filters were used for aerosol collection in our work, and they were acid-washed before being used for aerosol sampling to reduce background levels (Zhang et al., 2022). A total of 126 and 106 pairs of aerosol samples were collected at Xi'an and Qingdao, respectively (Zhang et al., 2023; Chen et al., 2024). After collection, all the aerosol samples were stored at -20°C for further analysis.

In addition to aerosol particles, we also sampled atmospheric acidic and alkaline gases (mainly NH₃, HCl and HNO₃) at Qingdao, using a ChemComb 3500 Speciation Collection Cartridge (Thermo Fisher Scientific, USA) at a flow rate of 10 L/min (Walters and Hastings, 2018; Fang et al., 2025). Gas sampling was carried out concurrently with aerosol sampling. In brief, NH₃, HNO₃ and HCl were absorbed onto the inner walls of two tandem honeycomb diffusion tubes coated with proper adsorbents, and then converted into NH₄⁺, NO₃⁻ and Cl⁻. After the sampling was completed, 20 mL ultrapure water was used to rinse each tube immediately, and a PTFE membrane syringe filter (0.22 μm in pore size) was used to filter the solution. The solution was then frozen at -20°C for further analysis.

2.2 Sample analysis and aerosol acidity calculation

Sample pretreatment and analysis were detailed in our previous work (Zhang et al., 2022), and therefore are only briefly summarized here. The first half of a filter (and only one quarter of a filter for supermicron particles) was shredded and digested in a Teflon jar using a microwave digestion instrument. After digestion, the Teflon jar was filled with 1% HNO₃ (20 mL), and a PTFE membrane syringe filter (0.22 µm in pore size) was used to filter the solution; subsequently, the solution was analyzed by inductively coupled plasma-mass spectrometry (ICP-MS) to determine total concentrations of individual trace elements, including Al.

The other half of a filter was immersed in ultrapure water (20 mL) and stirred using an orbital shaking for two hours; in the next step, the solution was filtered using a PTFE membrane syringe filter (0.22 µm in pore size) and divided into two parts. The first solution was acidified to contain 1% HNO₃ and subsequently analyzed by ICP-MS to determine the concentrations of dissolved trace elements; the second solution was analyzed by ion chromatography (IC) to

quantify the concentration of water-soluble cations and anions.

The solutions obtained from honeycomb diffusion tubes (see Section 2.1 for more details) were also analyzed using IC to determine the concentrations of gaseous NH₃, HCl and HNO₃ in the atmosphere. ISORROPIA-II, a widely used aerosol thermodynamic model (Fountoukis and Nenes, 2007), was employed in this work to calculate the acidity of supermicron and submicron particles. It was operated in the forward mode, and aerosol particles were assumed to remain metastable. Input parameters included concentrations of water-soluble ions in aerosol particles and gaseous NH₃, HCl and HNO₃, temperature and relative humidity (RH). Our previous work found good agreement between measured and calculated NH₃ partitioning coefficients at Qingdao (Fang et al., 2025), and as a result the method we used could well estimate the acidity of supermicron and submicron particles.

3. Results

3.1 Seasonal variations of total and dissolved aerosol Al

3.1.1 Total aerosol Al

Figure 2 displays seasonal variations of total and dissolved aerosol Al at Xi'an and Qingdao. At Xi'an (Figure 2a), total Al in supermicron particles showed highest concentrations in spring and winter $(1.54\pm0.89 \text{ and } 1.91\pm0.93 \text{ }\mu\text{g/m}^3)$ and lowest concentrations in summer $(0.96\pm0.54 \text{ }\mu\text{g/m}^3)$; a similar seasonal pattern was observed for submicron particles, with total Al concentrations being highest in spring and winter $(4.29\pm3.70 \text{ and } 2.92\pm1.47 \text{ }\mu\text{g/m}^3)$ and lowest in summer $(0.95\pm0.44 \text{ }\mu\text{g/m}^3)$. At Qingdao (Figure 2b), total Al concentrations in supermicron particles were highest in spring $(1.04\pm1.12 \text{ }\mu\text{g/m}^3)$ and lowest in summer and autumn $(0.33\pm0.18 \text{ and } 0.31\pm0.12 \text{ }\mu\text{g/m}^3)$; similarly, for submicron particles, total Al

concentrations were also highest in spring $(1.88\pm2.51~\mu\text{g/m}^3)$ and lowest in summer and autumn $(0.35\pm0.22~\text{and}~0.65\pm0.82~\mu\text{g/m}^3)$. For each season the median concentration of total aerosol Al was usually higher in submicron particles than supermicron particles at both locations (and there were some exceptions, as shown in Figures 1a and 1b). This is related to size dependence of mineralogy and elemental compositions of mineral dust aerosol, which is not well studied and deserves further investigation.

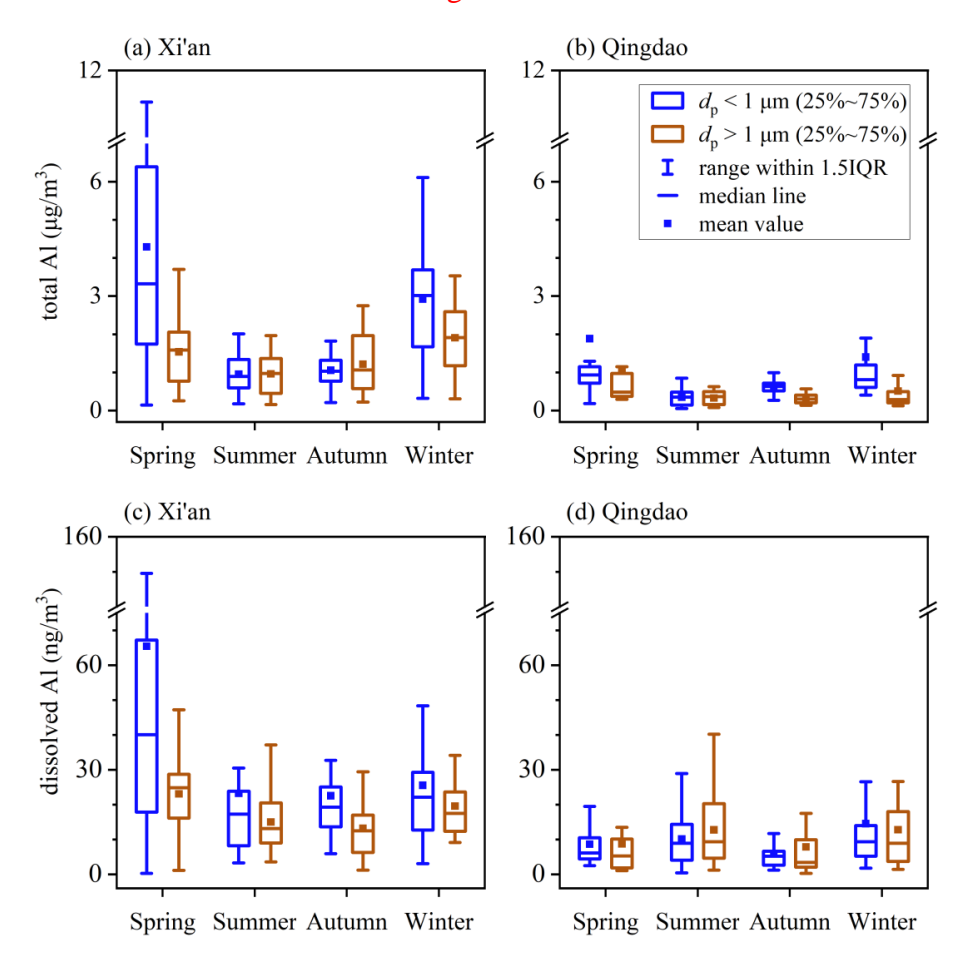


Figure 2. Seasonal variations of total and dissolved aerosol Al for submicron and supermicron particles: (a) total Al at Xi'an; (b) total Al at Qingdao; (c) dissolved Al at Xi'an; (d) dissolved Al at Qingdao.

Overall, total aerosol Al concentrations showed similar seasonal variations at Xi'an and

Qingdao, being highest in spring and lowest in summer. This was consistent with previous studies carried out in other locations in East Asia, such as Zhengzhou (Wang et al., 2019), Beijing (Zhang et al., 2013), Huaniao Island in the East China Sea (Guo et al., 2014), and Japan (Sakata et al., 2023). In East Asia, mineral dust aerosol was emitted into the atmosphere mainly in spring, leading to the increase in total aerosol Al concentrations. Lowest concentrations of total aerosol Al were observed in summer because precipitation in Northern China mainly occurred in summer, leading to enhanced wet deposition of aerosol particles (Cao and Cui, 2021). Furthermore, Qingdao was frequently affected by marine air masses in summer, and this is also one reason why total aerosol Al concentrations were lower in summer than other seasons. Total aerosol Al concentrations were higher in winter than summer and autumn at Xi'an, and one major reason is that meteorological conditions favored the accumulation of aerosol particles (including aerosol Al) during winter (Cao and Cui, 2021).

As summarized in the supplement (Table S2), total aerosol Al concentrations exhibited evident spatial variations in East Asia. As Asian dust was transported eastward to the North Pacific, a clear decrease in aerosol Al concentrations was observed. Mineral dust was the dominant source for aerosol Al, and therefore concentrations of aerosol Al were found to be very high in desert regions. For example, total Al concentrations in TSP could reach 24 µg/m³ over the Taklimakan Desert (Zhang et al., 2003). In our current study, annual average total Al concentrations at Xi'an, an inland city close to the desert, were reported to be 1.42±0.86 and 2.28±2.35 µg/m³ for supermicron and submicron particles, much lower than that observed over the Taklimakan Desert. Further decrease in total Al concentrations was observed in coastal and oceanic regions. For example, our work found that the annual average total Al concentrations

were 0.56 ± 0.75 and $1.08\pm1.67~\mu g/m^3$ for supermicron and submicron particles at Qingdao, lower than those at Xi'an; total Al concentrations in TSP ranged from 0.17 to $1.72~\mu g/m^3$ in Hiroshima (Sakata et al., 2023), and further decreased to $1\text{-}56~n g/m^3$ in Hawaii in the central Pacific (Measures et al., 2010).

3.1.2 Dissolved aerosol Al

At Xi'an (Figure 2c), for supermicron particles, dissolved aerosol Al concentrations were highest in spring (23.1±10.9 ng/m³) and lowest in summer and autumn (15.0±8.7 and 13.2±8.6 ng/m³); for submicron particles, dissolved Al concentrations were also highest in spring (65.4±79.2 ng/m³) and lowest in summer and autumn (23.2±23.4 and 22.6±20.1 ng/m³). Total (Figure 2a) and dissolved aerosol Al (Figure 2c) showed similar seasonal patterns at Xi'an, indicating that dissolved aerosol Al was mainly regulated by total aerosol Al.

As shown in Figure 2d, the average dissolved aerosol Al concentrations were 8.8±10.8, 12.8±11.1, 7.9±10.5 and 12.8±12.9 ng/m³ for supermicron particles at Qingdao in spring, summer, autumn, and winter, respectively, and 8.7±5.8, 10.2±8.2, 6.0±4.8 and 14.5±15.2 ng/m³ for submicron particles. Dissolved aerosol Al concentrations were highest in summer and winter and lowest in autumn for both supermicron and submicron particles. In contrast to Xi'an, total and dissolved aerosol Al at Qingdao showed different seasonal patterns (Figures 2b and 2d); for example, total Al concentrations were lowest in summer at Qingdao when dissolved Al concentrations were highest. This indicates that dissolved aerosol Al at Qingdao was not only regulated by total aerosol Al but also affected by other factors such as atmospheric aging processes.

Compared to Xi'an, dissolved Al concentrations at Qingdao were lower across all the four

seasons, mainly because total Al concentrations were much lower at Qingdao (Tables S3-S4 in the supplement). As shown in Figure 2, similar seasonal patterns were observed at two locations for total aerosol Al, but dissolved aerosol Al showed very different seasonality; this suggests that seasonal patterns of aerosol Al solubility were different at Xi'an and Qingdao, as presented in Section 3.2.

3.2 Fractional solubility of aerosol Al

3.2.1 Seasonal variations of Al solubility

Figure 3 displays aerosol Al solubility in different seasons at Xi'an and Qingdao. The median solubilities of aerosol Al were determined to be 1.38%, 1.59%, 1.04% and 1.01% for supermicron particles at Xi'an in spring, summer, autumn and winter, respectively, and 1.01%, 1.69%, 1.82% and 0.74% for submicron particles. Aerosol Al solubilities were generally low for the four seasons at Xi'an, showing no apparent variation with seasons (Figure 3a). In contrast, aerosol Al solubilities exhibited distinct seasonal variability at Qingdao (Figure 3b), and the median Al solubilities were highest in summer (3.56% and 2.33%) and lowest in spring (0.54% and 0.61%) for both supermicron and submicron particles.

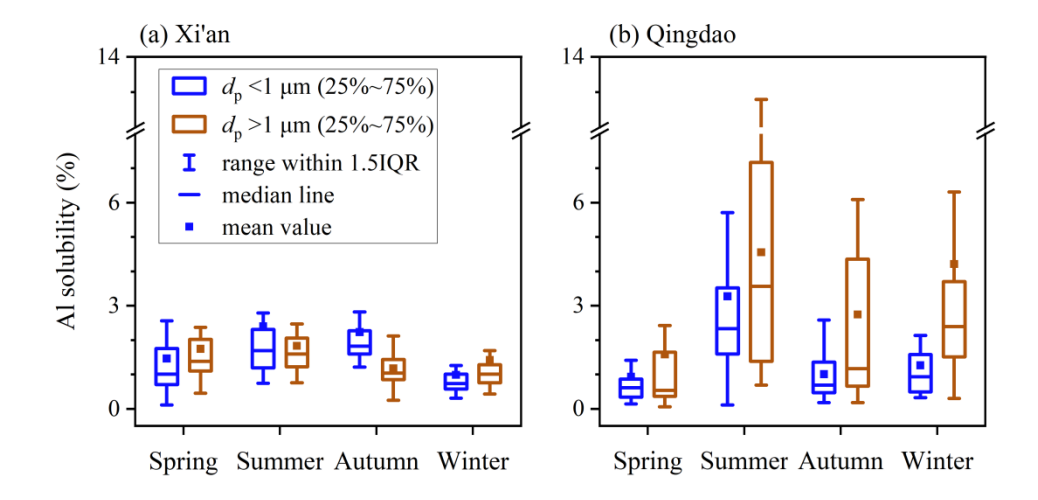


Figure 3. Seasonal variations of aerosol Al solubility for submicron and supermicron particles

In three seasons (summer, autumn and winter), aerosol Al solubility at Qingdao was higher than that at Xi'an (Figure 3, Table S5). There are several important dust sources in Northwest China, being far from (up to a few thousand km) or close to Xi'an. More importantly, anthropogenic emission in Northwest China is much smaller than the North China Plain, and thus the aging extent of mineral dust transported to Xi'an was rather limited (Wang et al., 2014; Wu et al., 2017). On the contrary, Qingdao is much farther from deserts; consequently, after long-distance transport over the North China Plain where anthropogenic emission is very large, mineral dust aerosol which arrived at Qingdao was substantially aged (Trochkine et al., 2003; Takahashi et al., 2011; Jeong, 2020), thereby leading to enhanced dissolution of aerosol Al and thus the increase in Al solubility. Mineral dust from different desert regions and local suspended dust cannot explain higher Al aerosol solubility observed at Qingdao, as previous work showed that Al solubility was low for soil samples from different regions (Shi et al., 2011; Wuttig et al., 2013; Aghnatios et al., 2014; Li et al., 2022; Hsieh et al., 2023).

On the other hand, no obvious difference in aerosol Al solubility was observed between Xi'an and Qingdao in spring, with median aerosol Al solubilities being <1.4% for supermicron and submicron particles (Figure 3). This agrees with a previous study (Hsu et al., 2010) which found that aerosol Al solubility was very low (average: ~0.7%) in spring even over the East China Sea. Furthermore, similar to what we observed in spring at Xi'an and Qingdao, Al solubility was found to be low (<1.5%) for surface soil particles collected from deserts (Shi et al., 2011; Aghnatios et al., 2014; Li et al., 2022). Overall, our work implies that in spring when

Asian dust occurred most frequently, mineral dust particles arriving at Qingdao after longdistance transport did not show substantial increase in Al solubility.

3.2.2 Al solubility under different weather conditions

We encountered four representative weather conditions (i.e. clean, dust, haze and fog days) during our sampling at Xi'an and Qingdao, and investigated aerosol Al solubility under different weather conditions (Figure 4, Tables S6-S7).

At Xi'an, no apparent difference in Al solubility was observed during clean, haze, and dust days (Figure 4a, Table S6), with median values in the range of 1.01-1.47% for supermicron particles and 0.72-1.86% for submicron particles. Al solubility was found to be <1.2% for three mineral dust samples (Luochuan loess, Arizona test dust, and dust collected during a dust storm in Xinjiang) (Li et al., 2022), and ranged from 0.47% to 1.42% for aerosol particles generated using soil samples from Saharan desert (Shi et al., 2011). Compared to mineral dust in source regions, Al solubility was not higher under different weather conditions at Xi'an. In addition, although emission and accumulation of anthropogenic pollutants was greatly enhanced during haze days at Xi'an (An et al., 2019; Cao and Cui, 2021), there was no obvious increase in aerosol Al solubility, indicating that the effects of anthropogenic emissions on aerosol Al solubility was limited at Xi'an. Therefore, one may conclude that aerosol Al solubility at Xi'an was not different from initial Al solubility of mineral dust.

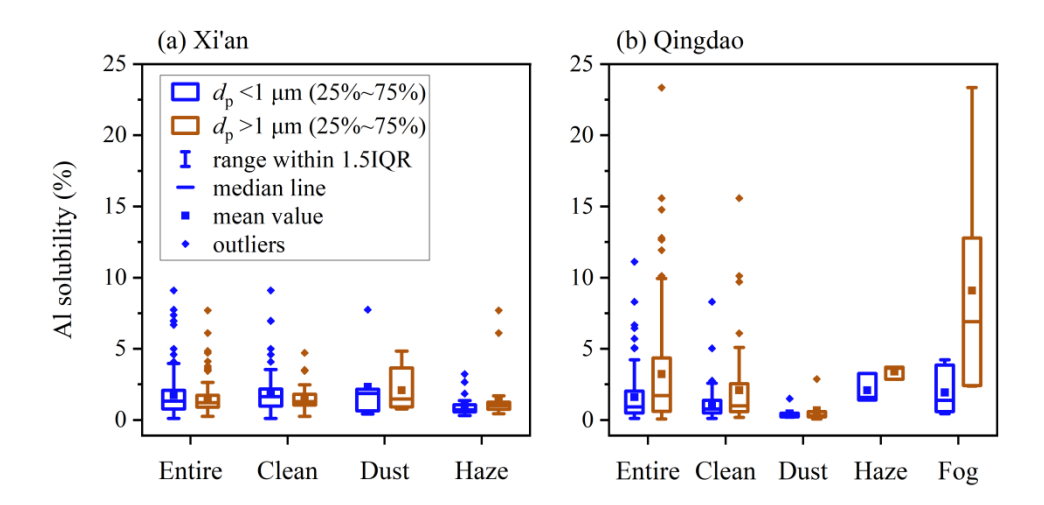


Figure 4. Aerosol Al solubility under different weather conditions for submicron and supermicron particles: (a) Xi'an, (b) Qingdao.

Being different to Xi'an, aerosol Al solubility at Qingdao shows remarkable variations under different weather conditions (Figure 4b, Table S7). Median Al solubilities were determined to be 0.31% and 0.24% for supermicron and submicron particles during dust days, lower than these on clean days (0.99% and 0.77%, respectively). This is probably because higher wind speeds during dust events hindered the accumulation of atmospheric pollutants and shortened the transport time to Qingdao, and thus limiting the aging of mineral dust aerosol. This explanation is supported by a recent study (Zhang et al., 2024) which found that the aging extent of dust particles in Japan was much lower during fast-moving dust events than slow-moving dust events. Moreover, large amounts of alkaline components (such as carbonates) which were emitted to the atmosphere during dust days neutralized acid species and therefore inhibited acid-promoted dissolution of aerosol trace elements (Zhi et al., 2025).

Figure 4b also suggests that aerosol Al solubilities were much higher during haze and fog days at Qingdao, when compared to clean days. Highest Al solubilities were observed during

fog days, with median values being 6.90% for supermicron particles and 1.38% for submicron particles, followed by haze days (3.64% and 1.58%, respectively). This is very likely due to enhanced chemical processing during haze and fog periods (Shi et al., 2020; Shang et al., 2024), and especially during fog days the large increase in RH cause huge increase in aerosol liquid water, therefore greatly promoting aqueous reactions and Al dissolution. Acid and ligand processing can both enhance aerosol Al solubility, although at present it is difficult to disentangle their individual contributions.

In summary, aerosol Al solubility at Xi'an was low in general, and did not show much variability in different seasons or under different weather conditions. Compared to Xi'an, aerosol Al solubility was higher at Qingdao; furthermore, it was higher in the other three seasons than in spring, and much higher for haze and fog days than dust days. These results imply that atmospheric aging had little effects on aerosol Al solubility at Xi'an but could remarkably increase aerosol Al solubility at Qingdao, as further elaborated in Section 4.

4. Discussion

As shown in Figure 5, our work observed the inverse dependence of aerosol Al solubility on total Al concentrations at both Xi'an and Qingdao, given by Eq. (1):

$$f_{s}(Al) = a \times [Al]^{-b} \tag{1}$$

where $f_s(Al)$ is aerosol Al solubility (%) and [Al] is total Al concentration (ng/m³). Such relationship was also reported in some previous studies (Jickells et al., 2016; Shelley et al., 2018; Baker et al., 2020; Shelley et al., 2025). Baker and Jickells (2006) suggested that such inverse relationship was due to that larger particles have higher deposition velocities and lower Al solubility: aerosol Al concentrations decrease during transport in the atmosphere due to

deposition, with deposition being faster for larger particles; as a result, aerosol particles will be enriched with smaller particles with higher Al solubility. However, Shi et al. (2011) found no substantial change in Al solubility with particle size for mineral dust samples, and therefore put the explanation proposed by Baker and Jickells (2006) into doubt.

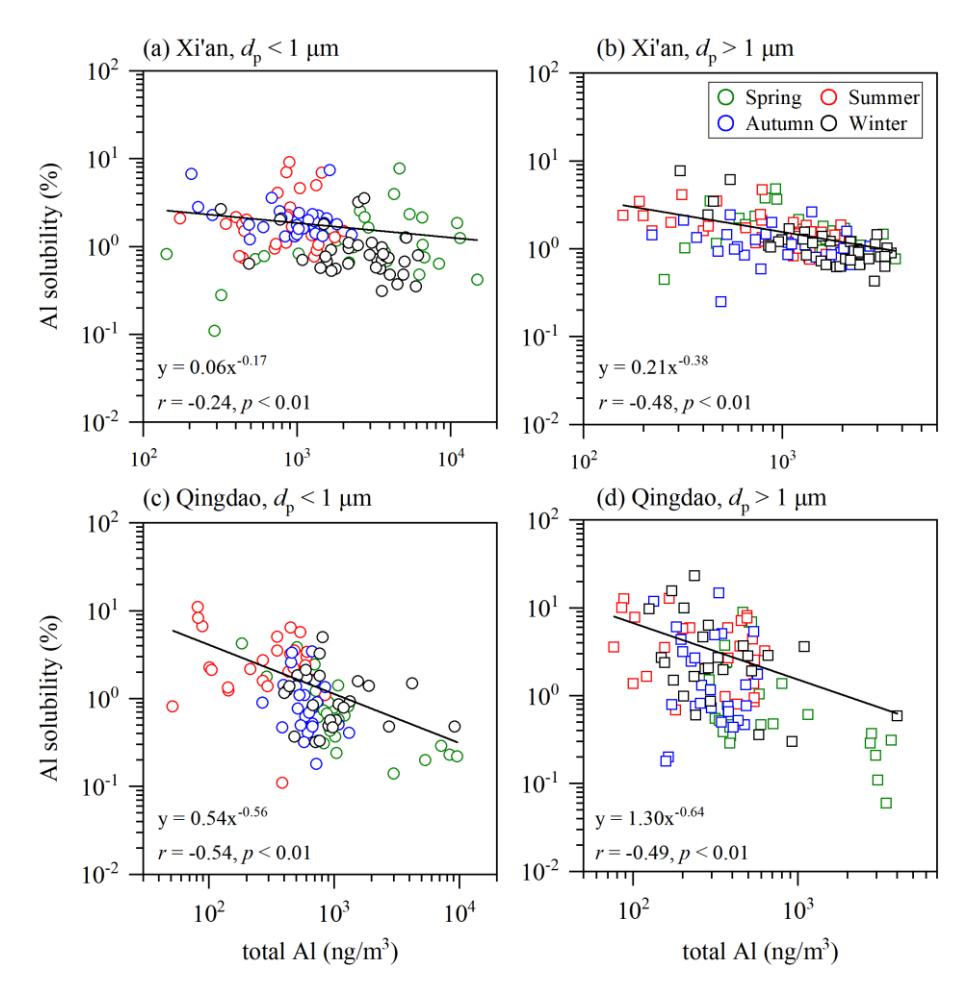


Figure 5. Aerosol Al solubility versus total aerosol Al concentrations: (a) submicron particles at Xi'an, (b) supermicron particles at Xi'an, (c) submicron particles at Qingdao, (d) supermicron particles at Qingdao.

Aerosol Fe solubility was also frequently observed to increase with the decrease in total Fe concentrations (Sedwick et al., 2007; Mahowald et al., 2018; Meskhidze et al., 2019), and

one possible reason is the influence of anthropogenic aerosol Fe (Sholkovitz et al., 2009; Ito and Shi, 2016) with higher solubility than mineral dust (Schroth et al., 2009; Fu et al., 2012; Ito et al., 2021). Nevertheless, being different from aerosol Fe, aerosol Al stems predominantly from mineral dust, with little contribution from anthropogenic sources; furthermore, Al solubility was measured to be 0.4±0.6% for coal fly ash (Li et al., 2022), an important type of anthropogenic aerosols, not higher than that for mineral dust (0.8±0.4%). Therefore, we suggest that anthropogenic emission may not be able to explain the inverse dependence of Al aerosol solubility on total Al concentrations.

We argue that chemical processing in the atmosphere can very well explain such inverse dependence. Total aerosol Al concentrations decrease with transport due to deposition, while reactions with acidic gases (such as SO₂ and NO_x) can enhance the dissolution of aerosol Al (Jickells et al., 2016). Figure 5 shows that the inverse dependence of Al solubility on total Al concentration was more pronounced at Qingdao, with the slopes (*b* values) much larger than those obtained at Xi'an. This is because compared to Xi'an, Qingdao is more distant from deserts and therefore dust aerosol is expected to be more aged at Qingdao. It also further supports the vital role chemical aging plays in regulating aerosol Al solubility,

4.1 Effects of acid processing and the role of RH

4.1.1 Effects of acid processing

Laboratory experiments found that the amount of Al dissolved from minerals would increase with the decrease in solution pH (Amram and Ganor, 2005; Bibi et al., 2011, 2014; Cappelli et al., 2018), and some field measurements also suggested that acid processing in the atmosphere could lead to large increase in aerosol Al solubility (Measures et al., 2010; Sakata

et al., 2023). In this work, we examined the relationship between aerosol Al solubility and the relative abundance of acidic species ([sulfate]/[Al] and [nitrate]/[Al]) at Xi'an and Qingdao. It should be noted that non-sea-salts sulfate (Virkkula et al., 2006), instead of sulfate, was used at Qingdao because it is a coastal city and heavily impacted by sea spray aerosol.

At Xi'an, overall aerosol Al solubility showed no significant correlation with [sulfate]/[Al] or [nitrate]/[Al] for either supermicron or submicron particles (r < 0.4, Figure 6 and S1), indicating that acid processing did not enhance aerosol Al solubility. Enhancement of aerosol trace element solubility by acid processing requires internal mixing of acid species with mineral dust particles (Baker and Croot, 2010). Previous studies suggested that mineral dust particles observed at Xi'an which is close to deserts largely remained externally mixed with acid species (Wang et al., 2014; Wu et al., 2017), and thus aerosol Al solubility was not apparently enhanced by acid processing at Xi'an.

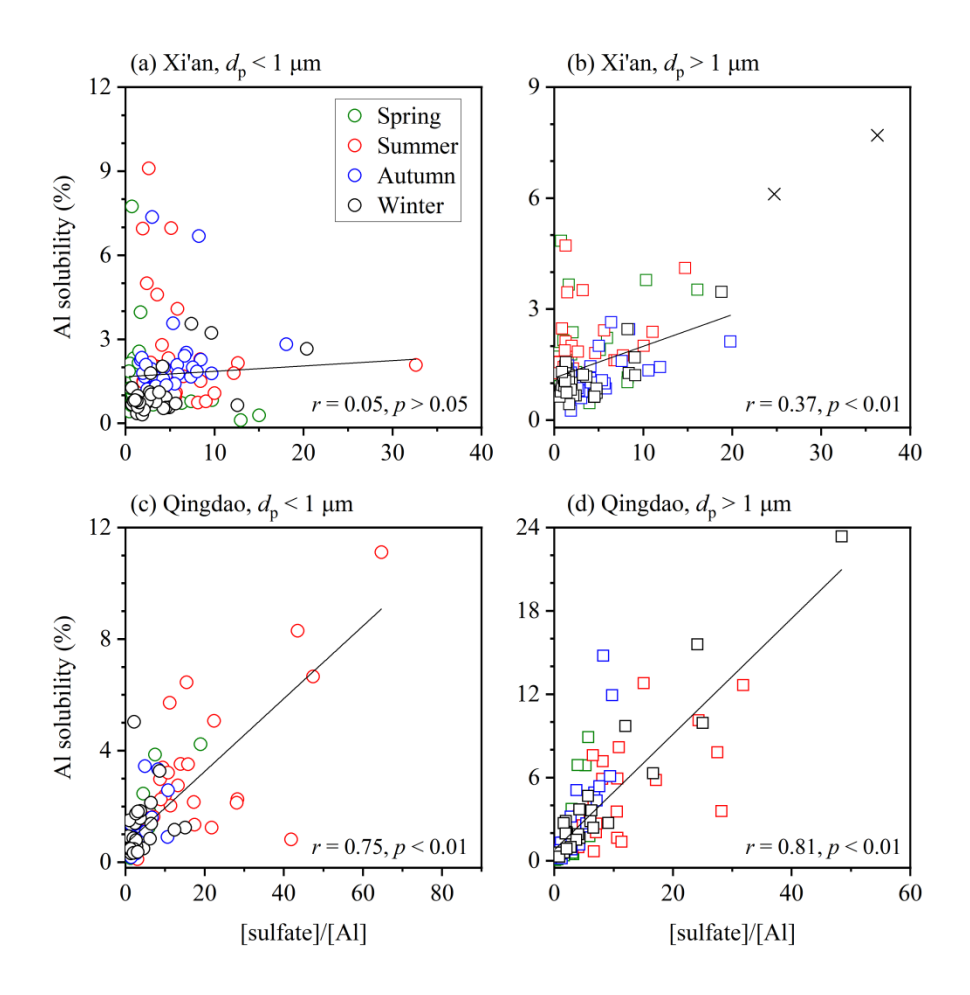


Figure 6. Aerosol Al solubility versus [sulfate]/[Al]: (a) submicron particles at Xi'an, (b) supermicron particles at Xi'an, (c) submicron particles at Qingdao, (d) supermicron particles at Qingdao. Data represented by crosses are not included in fitting.

On the contrary, Figure 6 shows that aerosol Al solubility at Qingdao was well correlated with [sulfate]/[Al] (r > 0.7, p < 0.01), implying that acid-promoted dissolution significantly enhanced Al solubility. We also found that correlations of Al solubility with [sulfate]/[Al] was better than those with [nitrate]/[Al] (Figures 6 and S1, Table S8), in line with a previous study (Sakata et al., 2023) which found aerosol Al solubility at Hiroshima, southern Japan, to be correlated with [sulfate]/[Al] but not with [nitrate]/[Al]. This may imply that chemical

processing by sulfate was more important than nitrate for Al solubility enhancement via acid processing, likely because aluminosilicate dust particles tend to react preferentially with SO₂ and H₂SO₄ while nitrogen oxides react mainly with carbonate particles (Sullivan et al., 2007; Fitzgerald et al., 2015). Furthermore, our work reveals better correlations between Al solubility and [sulfate]/[Al] for supermicron particles than submicron particles (Figure 6), indicating that the effect of acid processing on Al solubility was more important in supermicron particles.

4.1.2 The role of RH

Relative humidity (RH) is a vital factor influencing liquid water contents and phase state of aerosol particles and thus their secondary chemistry. When RH increased >60%, the phase state of aerosol particles in northern China changed from semisolid to liquid (Liu et al., 2017; Sun et al., 2018; Song et al., 2022), leading to large increase in aerosol liquid water content and thereby potentially affecting aerosol Al solubility.

We observed no apparent variation of aerosol Al solubility with RH at Xi'an (Figure 7a). When RH was <60%, median Al solubilities for supermicron and submicron particles were 1.22% and 1.14%, respectively; when RH increased >90%, the median Al solubilities were determined to be 1.82% and 0.82%, showing no obvious increase when compared to those at <60% RH. This again may imply that chemical processing had very limited impact on aerosol Al solubility at Xi'an, as mineral dust particles mostly remained externally mixed with secondary species and their aging extent was very limited (Wang et al., 2014; Wu et al., 2017).

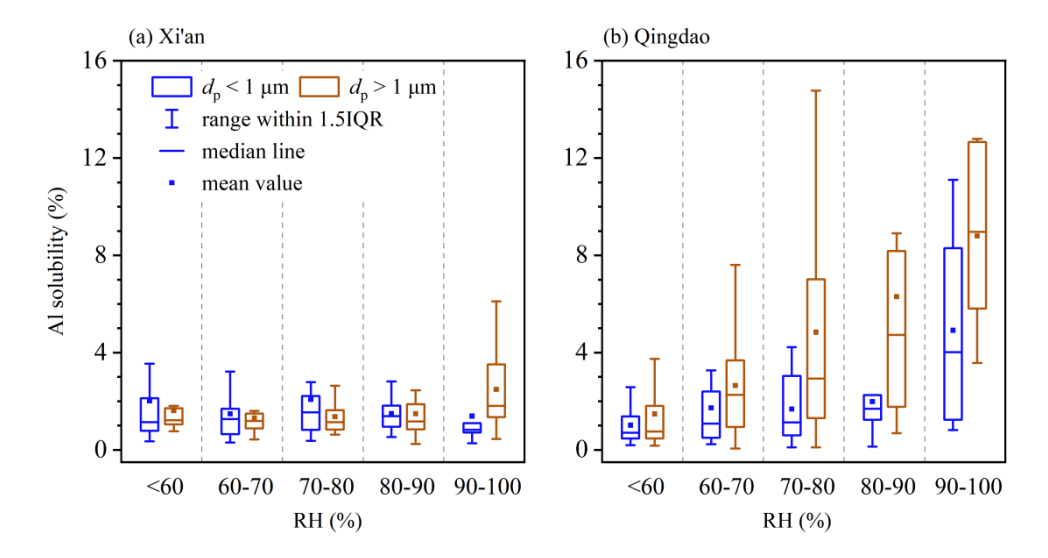


Figure 7. Aerosol Al solubility at different relative humidity (RH) for submicron and supermicron particles: (a) Xi'an, (b) Qingdao.

In contrast, RH played an important role in regulating aerosol Al solubility at Qingdao, because mineral dust particles observed at Qingdao had been transported through the North China Plain and were substantially aged. As shown in Figure 7b, for supermicron particles, the median Al solubility was only 0.76% at <60% RH, and gradually increased to 4.73% at 80-90% RH, and abruptly increased to 8.87% at >90% RH. For submicron particles, median Al solubility was <1% at <60% RH, and further increase in RH to 80-90% did not lead to large changes in Al solubility; nevertheless, when RH exceeded 90%, the median Al solubility was remarkably increased to 4.02%, much higher than those observed when RH was < 90%.

4.2 Effects of aerosol acidity on aerosol Al solubility at Qingdao

Figure 8 shows the dependence of aerosol Al solubility on aerosol acidity (represented by pH) at Qingdao (we did not measure NH₃ at Xi'an and thus could not estimate the aerosol acidity in a reliable manner). For supermicron particles, the median Al solubility was only 0.99%

when aerosol pH was >4.0, and gradually increased to 10.24% as aerosol pH was decreased to <2.5. For submicron particles, the median Al solubility was only 0.69% when pH was >4.0, increased slightly with the decrease in pH when pH was in the range of 2.5-4.0, and then increased greatly to 6.09% when pH was decreased to <2.5. In addition, aerosol acidity at Qingdao was highest in summer and lowest in spring (Chen et al., 2024), consistent with the seasonal variation of aerosol Al solubility, further supporting the importance of aerosol acidity in regulating Al solubility.

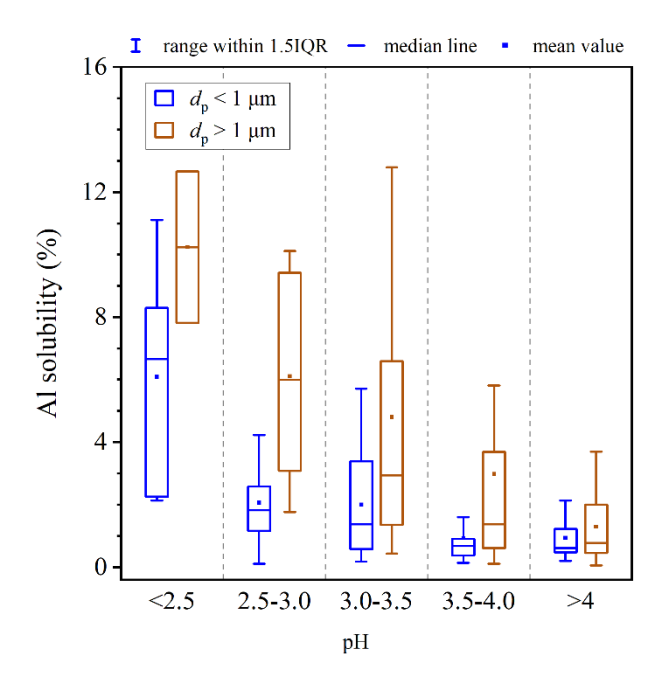


Figure 8. Aerosol Al solubility corresponding to different aerosol acidity for submicron and supermicron particles in Qingdao.

As shown in Figure S2, aerosol Al solubility was generally <2% when aerosol acidity was low (pH > 4.0), and higher Al solubility (>2%) was usually observed for samples with high RH and high acidity (pH < 4.0), again underscoring the roles of aerosol acidity (and RH). However, some samples exhibited low Al solubility although the corresponding RH and aerosol acidity

were both higher, and such phenomenon was more pronounced for submicron particles. This is very likely linked with aerosol mixing state (Riemer et al., 2019). Aerosol Al solubility and acidity used in our work are both the average properties of an aerosol sample which contains numerous particles, while in reality the two properties will have large particle-to-particle variations. For a given aerosol sample, it can happen that particles with high acidity may contain very little Al while particles with low acidity are enriched in Al; in this case, high acidity do not promote Al solubility for this sample. Single particle analysis which provides mixing state information can give further insights. We also note that samples with low Al solubility but high RH and high acidity were mostly found in clean days, perhaps due to the influence of local resuspended dust for which chemical aging was very limited.

4.3 Size-dependence of aerosol Al solubility

At Xi'an, no obvious difference in aerosol Al solubility was found between supermicron and submicron particles across all the four seasons (Figure 3a). This is because the aging extent of dust particles was rather limited at Xi'an (Wang et al., 2014; Wu et al., 2017) and Al solubility does not vary with particle size for unaged dust particles (Shi et al., 2011). At Qingdao, aerosol Al solubility showed no obvious difference between supermicron and submicron particles in spring, because the aging extent of dust arriving at Qingdao was also limited in spring when Asian dust occurred most frequently. However, in the other three seasons, Al solubility was higher for supermicron particles than submicron particles at Qingdao, and the ratios of median Al solubility in supermicron particles to that in submicron particles were found to be 1.53, 1.70 and 2.57 in summer, autumn and winter, respectively. Similar to

our observation at Qingdao, Li et al. (2017) found that aerosol Al solubility was much higher for TSP (14-28%) than $PM_{2.5}$ (2-23%) at the summit of Mount Heng, southern China.

448

449

450

451

452

453

454

455

456

457

458

459

460

461

462

463

464

465

466

467

468

469

On the other hand, a few other studies (Baker et al., 2020; Hsieh et al., 2023; Sakata et al., 2023; Yang et al., 2023) found that aerosol Al solubility was higher in fine particles than coarse particles. For example, aerosol Al solubility was found to increase with the decrease in particle size over the tropical eastern Atlantic (Baker et al., 2020), being ~10.31% for particles in the size of 0.36-0.61 µm and 0.43-4.53% for particles above 0.61 µm. At Hiroshima, southern Japan, aerosol Al solubility was reported to be 8.82±6.48% for fine particles (<1.3 μm), more than two times larger than that $(3.25\pm3.41\%)$ for coarse particles (>1.3 µm) (Sakata et al., 2023). Baker and Jickells (2006) suggested that this is because fine particles have larger surface-tovolume ratios and thus facilitate Al dissolution via acid processing. Hsieh et al. (2023) found aerosol Al solubility to be 38% for fine particles (0.57-1.0 μm) but only 0.37% for coarse particles (>7.3 µm) over the East China Sea, and suggested that the observed size-dependence could be explained by the enrichment of anthropogenic Al (which has higher solubility than dust Al) in fine particles. However, aerosol Al originates predominantly from mineral dust, with little contributions from anthropogenic sources (Taylor and McLennan, 1985; Mahowald et al., 2018), and fractional solubility of anthropogenic Al was not necessarily higher than mineral dust (Li et al., 2022).

As discussed above, there is not clear yet how and why aerosol Al solubility varies with particle size. Such discrepancy is at least partly because different leaching protocols were used in previous studies to extract dissolved aerosol Al and thereby Al solubility obtained in different studies was not directly comparable (Meskhidze et al., 2019; Li et al., 2023; Li et al.,

2024). Furthermore, mechanistic insights can be obtained by laboratory experiments which examine the size dependence of the solubility and dissolution kinetics of Al for mineral dust particles under atmospherically relevant conditions.

5. Conclusions and atmospheric implications

Deposition of mineral dust aerosol is a major external source of several nutrient and toxic elements for surface water in open oceans, and thus have large impacts on marine biogeochemistry; however, previous studies which estimated dust deposition flux into the oceans reveals large discrepancies. Aerosol Al solubility, which is a critical parameter in using dissolved Al concentrations in surface seawater as a tracer to constrain dust deposition flux, remains poorly understood. In this work, we investigated seasonal variations of aerosol Al solubility for supermicron (>1 µm) and submicron (<1 µm) aerosol particles at Xi'an and Qingdao, both located in northern China, in attempt to elucidate the processes and mechanisms which govern the variation of aerosol Al solubility in the atmosphere.

At Xi'an, aerosol Al solubility was low in general for both supermicron and submicron particles, showing no obvious variability in different seasons or under different weather conditions. This implies that chemical processing did not substantially enhance aerosol Al solubility at Xi'an, as it is an inland city close to major deserts in northwestern China and thus the aging extent of mineral dust particles arriving at Xi'an was quite limited. Compared to Xi'an, aerosol Al solubility was higher at Qingdao, a coastal city in northern China; furthermore, Al solubility was higher in the other three seasons than in spring, and much higher for haze- and especially fog-impacted days than dust days. This indicates that chemical processing substantially increased aerosol Al solubility at Qingdao.

Aerosol Al solubility at Xi'an showed no significant correlation with relative abundance of sulfate or nitrate, and did not vary apparently with RH; in contrast, Al solubility at Qingdao was well correlated with relative abundance of sulfate and nitrate, and increased with RH. This further supports that chemical processing had little impacts on aerosol Al solubility at Xi'an (because the aging extent of mineral dust aerosol at Xi'an is very limited) but remarkably increased aerosol Al solubility at Qingdao (because mineral dust particles transported to Qingdao were substantially aged). Moreover, for both supermicron and submicron particles, Al solubility at Qingdao was found to increase with aerosol acidity (in addition to RH), underscoring the vital role of aerosol liquid water and acidity in enhancing Al dissolution via chemical aging.

Our comprehensive investigation of aerosol Al solubility at two locations in Northern China suggests that atmospheric chemical processing dictates aerosol Al solubility. As a result, aerosol Al solubility is expected to spatially variable, depending on the extent of chemical processing. For example, we found that aerosol Al solubility is higher at Qingdao than Xi'an in general, and expect it to increase further as mineral dust aerosol is further transported eastward to the Pacific. As a result, when leveraging dissolved Al concentrations in surface seawater as a tracer to estimate deposition flux of mineral dust aerosol into open oceans, considering the spatial distribution of aerosol Al solubility, instead of using a uniform value on the global scale, can help us better constrain the oceanic deposition flux of mineral dust.

Author contribution.

513	TZ: Formal analysis, Investigation, Writing - Original Draft, Writing - Review & Editing;
514	YC: Formal analysis, Investigation, Writing - Original Draft; HZ: Investigation; Lei Liu:
515	Writing - Review & Editing; CH: Investigation; ZF: Investigation; YZ: Investigation; FW:
516	Resources; Lan Luo: Resources; GZ: Writing - Review & Editing; XW: Resources; MT:
517	Conceptualization, Formal analysis, Supervision; Writing - Original Draft, Writing - Review
518	& Editing.
519	Competing interests.
520	The authors declare that they have no conflict of interest.
521	Acknowledgement.
522	We would like to thank colleagues at Shandong University, Shaanxi University of Science
523	and Technology, and Institute of Earth Environment, Chinese Academy of Sciences for their
524	support during field measurements.
525	Financial support.
526	This work was sponsored by National Natural Science Foundation of China (42277088,
527	42407149 and 22361162668), Guangzhou Bureau of Science and Technology
528	(2024A04J6533), International Partnership Program of Chinese Academy of Sciences
529	(164GJHZ2024011FN), Guangdong Basic and Applied Basic Research Fund Committee
530	(2023A1515012010), and Guangdong Foundation for Program of Science and Technology
531	Research (2023B1212060049).
532	

References

534

558

559

- Aghnatios, C., Losno, R., and Dulac, F.: A fine fraction of soil used as an aerosol analogue during the DUNE experiment: sequential solubility in water, decreasing pH step-by-step, Biogeosciences, 11, 4627-4633, https://doi.org/10.5194/bg-11-4627-2014, 2014.
- Amram, K., and Ganor, J.: The combined effect of pH and temperature on smectite dissolution rate under acidic conditions, Geochim. Cosmochim. Acta, 69, 2535-2546, https://doi.org/10.1016/j.gca.2004.10.001, 2005.
- An, Z., Huang, R., Zhang, R., Tie, X., Li, G., Cao, J., Zhou, W., Shi, Z., Han, Y., Gu, Z., and Ji, Y.: Severe haze in northern China: A synergy of anthropogenic emissions and atmospheric processes, PNAS, 116, 8657-8666, https://doi.org/10.1073/pnas.1900125116, 2019.
- Anderson, R. F., Cheng, H., Edwards, R. L., Fleisher, M. Q., Hayes, C. T., Huang, K. F., Kadko, D., Lam, P. J.,
 Landing, W. M., Lao, Y., Lu, Y., Measures, C. I., Moran, S. B., Morton, P. L., Ohnemus, D. C.,
 Robinson, L. F., and Shelley, R. U.: How well can we quantify dust deposition to the ocean?, Phil.
 Trans. R. Soc. A, 374: 20150285, https://doi.org/10.1098/rsta.2015.0285, 2016.
- Baker, A. R., and Jickells, T. D.: Mineral particle size as a control on aerosol iron solubility, Geophys. Res. Lett., 33, L17608, https://doi.org/10.1029/2006gl026557, 2006.
- Baker, A. R., Jickells, T. D., Witt, M., and Linge, K. L.: Trends in the solubility of iron, aluminium, manganese and phosphorus in aerosol collected over the Atlantic Ocean, Mar. Chem., 98, 43-58, https://doi.org/10.1016/j.marchem.2005.06.004, 2006.
- Baker, A. R., and Croot, P. L.: Atmospheric and marine controls on aerosol iron solubility in seawater, Mar. Chem., 120, 4-13, https://doi.org/10.1016/j.marchem.2008.09.003, 2010.
- Baker, A. R., Li, M., and Chance, R.: Trace Metal Fractional Solubility in Size Segregated Aerosols From the
 Tropical Eastern Atlantic Ocean, Global Biogeochem. Cycles, 34, e2019GB006510,
 https://doi.org/10.1029/2019gb006510, 2020.
 - Benaltabet, T., Lapid, G., and Torfstein, A.: Dissolved aluminium dynamics in response to dust storms, wet deposition, and sediment resuspension in the Gulf of Aqaba, northern Red Sea, Geochim. Cosmochim. Acta, 335, 137-154, https://doi.org/10.1016/j.gca.2022.08.029, 2022.
- Bibi, I., Singh, B., and Silvester, E.: Dissolution of illite in saline—acidic solutions at 25°C, Geochim. Cosmochim. Acta, 75, 3237-3249, https://doi.org/10.1016/j.gca.2011.03.022, 2011.
- Bibi, I., Singh, B., and Silvester, E.: Dissolution kinetics of soil clays in sulfuric acid solutions: Ionic strength
 and temperature effects, Appl. Geochem., 51, 170-183,
 https://doi.org/10.1016/j.apgeochem.2014.10.004, 2014.
- Buck, C. S., Landing, W. M., Resing, J. A., and Measures, C. I.: The solubility and deposition of aerosol Fe and other trace elements in the North Atlantic Ocean: Observations from the A16N CLIVAR/CO2 repeat hydrography section, Mar. Chem., 120, 57-70, https://doi.org/10.1016/j.marchem.2008.08.003, 2010.
- Buck, C. S., Landing, W. M., and Resing, J.: Pacific Ocean aerosols: Deposition and solubility of iron,
 aluminum, and other trace elements, Mar. Chem., 157, 117-130,
 https://doi.org/10.1016/j.marchem.2013.09.005, 2013.
- Cao, J. J., and Cui, L.: Current Status, Characteristics and Causes of Particulate Air Pollution in the Fenwei
 Plain, China: A Review, J. Geophys. Res.-Atmos., 126, e2020JD034472,
 https://doi.org/10.1029/2020JD034472, 2021.
- 575 Cappelli, C., Yokoyama, S., Cama, J., and Huertas, F. J.: Montmorillonite dissolution kinetics: Experimental and

- reactive transport modeling interpretation, Geochim. Cosmochim. Acta, 227, 96-122, https://doi.org/10.1016/j.gca.2018.01.039, 2018.
- 578 Chance, R., Jickells, T. D., and Baker, A. R.: Atmospheric trace metal concentrations, solubility and deposition 579 fluxes in remote marine air over the south-east Atlantic, Mar. Chem., 177, 45-56, 580 https://doi.org/10.1016/j.marchem.2015.06.028, 2015.
- Chen, Y., Wang, Z., Fang, Z., Huang, C., Xu, H., Zhang, H., Zhang, T., Wang, F., Luo, L., Shi, G., Wang, X., and
 Tang, M.: Dominant Contribution of Non-dust Primary Emissions and Secondary Processes to
 Dissolved Aerosol Iron, Environ. Sci. Technol., 58, 17355-17363,
 https://doi.org/10.1021/acs.est.4c05816, 2024.
- Fang, Z., Dong, S., Huang, C., Jia, S., Wang, F., Liu, H., Meng, H., Luo, L., Chen, Y., Zhang, H., Li, R., Zhu, Y., and Tang, M.: On using an aerosol thermodynamic model to calculate aerosol acidity of coarse particles, J. Environ. Sci., 148, 46-56, https://doi.org/10.1016/j.jes.2023.07.001, 2025.
- 588 Fitzgerald, E., Ault, A. P., Zauscher, M. D., Mayol-Bracero, O. L., and Prather, K. A.: Comparison of the mixing 589 state of long-range transported Asian and African mineral dust, Atmos. Environ., 115, 19-25, 590 https://doi.org/10.1016/j.atmosenv.2015.04.031, 2015.
- Fountoukis, C., and Nenes, A.: ISORROPIA II: a computationally efficient thermodynamic equilibrium model for K⁺-Ca²⁺-Mg²⁺-NH₄⁺-Na⁺-SO₄²⁻-NO₃⁻-Cl⁻-H₂O aerosols, Atmos. Chem. Phys., 7, 4639-4659, https://doi.org/10.5194/acp-7-4639-2007, 2007.
- Fu, H., Lin, J., Shang, G., Dong, W., Grassian, V. H., Carmichael, G. R., Li, Y., and Chen, J.: Solubility of Iron
 from Combustion Source Particles in Acidic Media Linked to Iron Speciation, Environ. Sci. Technol.,
 46, 11119-11127, https://doi.org/10.1021/es302558m, 2012.
- Grand, M. M., Measures, C. I., Hatta, M., Hiscock, W. T., Buck, C. S., and Landing, W. M.: Dust deposition in
 the eastern Indian Ocean: The ocean perspective from Antarctica to the Bay of Bengal, Global
 Biogeochem. Cycles, 29, 357-374, https://doi.org/10.1002/2014GB004898, 2015.
- Guo, L., Chen, Y., Wang, F., Meng, X., Xu, Z., and Zhuang, G.: Effects of Asian dust on the atmospheric input of trace elements to the East China Sea, Mar. Chem., 163, 19-27, https://doi.org/10.1016/j.marchem.2014.04.003, 2014.
- Han, Q., Moore, J. K., Zender, C., Measures, C., and Hydes, D.: Constraining oceanic dust deposition using
 surface ocean dissolved Al, Global Biogeochem. Cycles, 22, GB2003,
 https://doi.org/10.1029/2007GB002975, 2008.
- Hsieh, C.-C., You, C.-F., and Ho, T.-Y.: The solubility and deposition flux of East Asian aerosol metals in the
 East China Sea: The effects of aeolian transport processes, Mar. Chem., 253, 104268,
 https://doi.org/10.1016/j.marchem.2023.104268, 2023.
- Hsu, S.-C., Wong, G. T. F., Gong, G.-C., Shiah, F.-K., Huang, Y.-T., Kao, S.-J., Tsai, F., Candice Lung, S.-C.,
 Lin, F.-J., Lin, I. I., Hung, C.-C., and Tseng, C.-M.: Sources, solubility, and dry deposition of aerosol
 trace elements over the East China Sea, Mar. Chem., 120, 116-127,
 https://doi.org/10.1016/j.marchem.2008.10.003, 2010.
- Huneeus, N., Schulz, M., Balkanski, Y., Griesfeller, J., Prospero, J., Kinne, S., Bauer, S., Boucher, O., Chin, M.,
 Dentener, F., Diehl, T., Easter, R., Fillmore, D., Ghan, S., Ginoux, P., Grini, A., Horowitz, L., Koch, D.,
 Krol, M. C., Landing, W., Liu, X., Mahowald, N., Miller, R., Morcrette, J. J., Myhre, G., Penner, J.,
 Perlwitz, J., Stier, P., Takemura, T., and Zender, C. S.: Global dust model intercomparison in AeroCom
 phase I, Atmos. Chem. Phys., 11, 7781-7816, https://doi.org/10.5194/acp-11-7781-2011, 2011.
- Ito, A., and Shi, Z.: Delivery of anthropogenic bioavailable iron from mineral dust and combustion aerosols to

- the ocean, Atmos. Chem. Phys., 16, 85-99, https://doi.org/10.5194/acp-16-85-2016, 2016.
- Ito, A., Ye, Y., Baldo, C., and Shi, Z.: Ocean fertilization by pyrogenic aerosol iron, npj Clim. Atmos. Sci., 4, 30, https://doi.org/10.1038/s41612-021-00185-8, 2021.
- Jeong, G. Y.: Mineralogy and geochemistry of Asian dust: dependence on migration path, fractionation, and reactions with polluted air, Atmos. Chem. Phys., 20, 7411-7428, https://doi.org/10.5194/acp-20-7411-624
 2020, 2020.
- Jiang, H.-B., Hutchins, D. A., Zhang, H.-R., Feng, Y.-Y., Zhang, R.-F., Sun, W.-W., Ma, W., Bai, Y., Wells, M.,
 He, D., Jiao, N., Wang, Y., and Chai, F.: Complexities of regulating climate by promoting marine
 primary production with ocean iron fertilization, Earth Sci. Rev., 249, 104675,
 https://doi.org/10.1016/j.earscirev.2024.104675, 2024.
- Jickells, T. D., An, Z. S., Andersen, K. K., Baker, A. R., Bergametti, G., Brooks, N., Cao, J. J., Boyd, P. W.,
 Duce, R. A., Hunter, K. A., Kawahata, H., Kubilay, N., laRoche, J., Liss, P. S., Mahowald, N.,
 Prospero, J. M., Ridgwell, A. J., Tegen, I., and Torres, R.: Global Iron Connections Between Desert
 Dust, Ocean Biogeochemistry, and Climate, Science, 308, 67-71,
 https://doi.org/10.1126/science.1105959, 2005.
- Jickells, T. D., Baker, A. R., and Chance, R.: Atmospheric transport of trace elements and nutrients to the oceans, Phil. Trans. R. Soc. A, 374, 20150286, https://doi.org/10.1098/rsta.2015.0286, 2016.
- Kok, J. F., Storelvmo, T., Karydis, V. A., Adebiyi, A. A., Mahowald, N. M., Evan, A. T., He, C., and Leung, D.
 M.: Mineral dust aerosol impacts on global climate and climate change, Nat. Rev. Earth Environ., 4,
 71-86, https://doi.org/10.1038/s43017-022-00379-5, 2023.
- Li, R., Zhang, H., Wang, F., Ren, Y., Jia, S., Jiang, B., Jia, X., Tang, Y., and Tang, M.: Abundance and fractional solubility of phosphorus and trace metals in combustion ash and desert dust: Implications for bioavailability and reactivity, Sci. Total Environ., 816, 151495,
 https://doi.org/10.1016/j.scitotenv.2021.151495, 2022.
- Li, R., Dong, S., Huang, C., Yu, F., Wang, F., Li, X., Zhang, H., Ren, Y., Guo, M., Chen, Q., Ge, B., and Tang,
 M.: Evaluating the effects of contact time and leaching solution on measured solubilities of aerosol
 trace metals, Appl. Geochem., 148, 105551, https://doi.org/10.1016/j.apgeochem.2022.105551, 2023.
- Li, R., Panda, P. P., Chen, Y., Zhu, Z., Wang, F., Zhu, Y., Meng, H., Ren, Y., Kumar, A., and Tang, M.: Aerosol trace element solubility determined using ultrapure water batch leaching: an intercomparison study of four different leaching protocols, Atmos. Meas. Tech., 17, 3147-3156, https://doi.org/10.5194/amt-17-3147-2024, 2024.
- Li, T., Wang, Y., Zhou, J., Wang, T., Ding, A., Nie, W., Xue, L., Wang, X., and Wang, W.: Evolution of trace elements in the planetary boundary layer in southern China: Effects of dust storms and aerosol-cloud interactions, J. Geophys. Res.-Atmos., 122, 3492-3506, https://doi.org/10.1002/2016JD025541, 2017.
- Li, W., Shao, L., Shi, Z., Chen, J., Yang, L., Yuan, Q., Yan, C., Zhang, X., Wang, Y., Sun, J., Zhang, Y., Shen, X.,
 Wang, Z., and Wang, W.: Mixing state and hygroscopicity of dust and haze particles before leaving
 Asian continent, J. Geophys. Res.-Atmos., 119, 1044-1059, https://doi.org/10.1002/2013JD021003,
 2014.
- Liu, Y., Wu, Z., Wang, Y., Xiao, Y., Gu, F., Zheng, J., Tan, T., Shang, D., Wu, Y., Zeng, L., Hu, M., Bateman, A.
 P., and Martin, S. T.: Submicrometer Particles Are in the Liquid State during Heavy Haze Episodes in
 the Urban Atmosphere of Beijing, China, Environ. Sci. Technol. Lett., 4, 427-432,
 https://doi.org/10.1021/acs.estlett.7b00352, 2017.
- López-García, P., Gelado-Caballero, M. D., Collado-Sánchez, C., and Hernández-Brito, J. J.: Solubility of

- aerosol trace elements: Sources and deposition fluxes in the Canary Region, Atmos. Environ., 148, 167-174, https://doi.org/10.1016/j.atmosenv.2016.10.035, 2017.
- Mahowald, N.: Aerosol Indirect Effect on Biogeochemical Cycles and Climate, Science, 334, 794-796, https://doi.org/10.1126/science.1207374, 2011.
- Mahowald, N. M., Hamilton, D. S., Mackey, K. R. M., Moore, J. K., Baker, A. R., Scanza, R. A., and Zhang, Y.:
 Aerosol trace metal leaching and impacts on marine microorganisms, Nat. Commun., 9, 2614,
 https://doi.org/10.1038/s41467-018-04970-7, 2018.
- Measures, C. I., and Brown, E. T.: Estimating Dust Input to the Atlantic Ocean Using Surface Water Aluminium
 Concentrations, in: The Impact of Desert Dust Across the Mediterranean, edited by: Guerzoni, S., and
 Chester, R., Springer Netherlands, Dordrecht, 301-311, 1996.
- Measures, C. I., and Vink, S.: On the use of dissolved aluminum in surface waters to estimate dust deposition to the ocean, Global Biogeochem. Cycles, 14, 317-327, https://doi.org/10.1029/1999GB001188, 2000.
- Measures, C. I., Sato, T., Vink, S., Howell, S., and Li, Y. H.: The fractional solubility of aluminium from mineral aerosols collected in Hawaii and implications for atmospheric deposition of biogeochemically important trace elements, Mar. Chem., 120, 144-153, https://doi.org/10.1016/j.marchem.2009.01.014,
 2010.
- Meskhidze, N., Völker, C., Al-Abadleh, H. A., Barbeau, K., Bressac, M., Buck, C., Bundy, R. M., Croot, P.,
 Feng, Y., Ito, A., Johansen, A. M., Landing, W. M., Mao, J., Myriokefalitakis, S., Ohnemus, D.,
 Pasquier, B., and Ye, Y.: Perspective on identifying and characterizing the processes controlling iron
 speciation and residence time at the atmosphere-ocean interface, Mar. Chem., 217, 103704,
 https://doi.org/10.1016/j.marchem.2019.103704, 2019.
- Moore, C. M., Mills, M. M., Arrigo, K. R., Berman-Frank, I., Bopp, L., Boyd, P. W., Galbraith, E. D., Geider, R.
 J., Guieu, C., Jaccard, S. L., Jickells, T. D., La Roche, J., Lenton, T. M., Mahowald, N. M., Marañón,
 E., Marinov, I., Moore, J. K., Nakatsuka, T., Oschlies, A., Saito, M. A., Thingstad, T. F., Tsuda, A., and
 Ulloa, O.: Processes and patterns of oceanic nutrient limitation, Nature Geoscience, 6, 701-710,
 https://doi.org/10.1038/ngeo1765, 2013.
- Pan, X., Uno, I., Wang, Z., Nishizawa, T., Sugimoto, N., Yamamoto, S., Kobayashi, H., Sun, Y., Fu, P., Tang, X., and Wang, Z.: Real-time observational evidence of changing Asian dust morphology with the mixing of heavy anthropogenic pollution, Sci. Rep., 7, 335, https://doi.org/10.1038/s41598-017-00444-w, 2017.
 - Paris, R., Desboeufs, K. V., Formenti, P., Nava, S., and Chou, C.: Chemical characterisation of iron in dust and biomass burning aerosols during AMMA-SOP0/DABEX: implication for iron solubility, Atmos. Chem. Phys., 10, 4273-4282, https://doi.org/10.5194/acp-10-4273-2010, 2010.
- Prospero, J. M., Ginoux, P., Torres, O., Nicholson, S. E., and Gill, T. E.: Environmental characterization of
 global sources of atmospheric soil dust identified with the Nimbus 7 Total Ozone Mapping
 Spectrometer (TOMS) absorbing aerosol product, Rev. Geophys., 40, 2-1-2-31,
 https://doi.org/10.1029/2000RG000095, 2002.

692

- Riemer, N., Ault, A. P., West, M., Craig, R. L., and Curtis, J. H.: Aerosol Mixing State: Measurements,
 Modeling, and Impacts, Rev. Geophys., 57, 187-249, https://doi.org/10.1029/2018RG000615, 2019.
- Sakata, K., Sakaguchi, A., Yamakawa, Y., Miyamoto, C., Kurisu, M., and Takahashi, Y.: Measurement report:
 Stoichiometry of dissolved iron and aluminum as an indicator of the factors controlling the fractional solubility of aerosol iron results of the annual observations of size-fractionated aerosol particles in
 Japan, Atmos. Chem. Phys., 23, 9815-9836, https://doi.org/10.5194/acp-23-9815-2023, 2023.
- Schroth, A. W., Crusius, J., Sholkovitz, E. R., and Bostick, B. C.: Iron solubility driven by speciation in dust

- sources to the ocean, Nature Geoscience, 2, 337-340, https://doi.org/10.1038/ngeo501, 2009.
- Schulz, M., Prospero, J. M., Baker, A. R., Dentener, F., Ickes, L., Liss, P. S., Mahowald, N. M., Nickovic, S.,
 García-Pando, C. P., Rodríguez, S., Sarin, M., Tegen, I., and Duce, R. A.: Atmospheric Transport and
 Deposition of Mineral Dust to the Ocean: Implications for Research Needs, Environ. Sci. Technol., 46,
 10390-10404, https://doi.org/10.1021/es300073u, 2012.
- Sedwick, P. N., Sholkovitz, E. R., and Church, T. M.: Impact of anthropogenic combustion emissions on the fractional solubility of aerosol iron: Evidence from the Sargasso Sea, Geochem. Geophys. Geosyst., 8, https://doi.org/10.1029/2007GC001586, 2007.
- Shang, T., Kong, L., and Qi, J.: Metal elements in atmospheric aerosols during different pollution events in the coastal region of the Yellow Sea: Concentration, solubility and deposition flux, Mar. Pollut. Bull., 206, 116711, https://doi.org/10.1016/j.marpolbul.2024.116711, 2024.
- Shelley, R. U., Landing, W. M., Ussher, S. J., Planquette, H., and Sarthou, G.: Regional trends in the fractional solubility of Fe and other metals from North Atlantic aerosols (GEOTRACES cruises GA01 and GA03) following a two-stage leach, Biogeosciences, 15, 2271-2288, https://doi.org/10.5194/bg-15-2271-2018, 2018.
- Shelley, R. U., Baker, A. R., Thomas, M., and Murphy, S.: Aerosol trace element solubility and deposition fluxes
 over the Mediterranean Sea and Black Sea basins, Biogeosciences, 22, 585-600,
 https://doi.org/10.5194/bg-22-585-2025, 2025.
- Shi, J., Guan, Y., Ito, A., Gao, H., Yao, X., Baker, A. R., and Zhang, D.: High Production of Soluble Iron Promoted by Aerosol Acidification in Fog, Geophys. Res. Lett., 47, e2019GL086124, https://doi.org/10.1029/2019GL086124, 2020.

727

728

729

730

731

732

733

734

735

- Shi, Z. B., Woodhouse, M. T., Carslaw, K. S., Krom, M. D., Mann, G. W., Baker, A. R., Savov, I., Fones, G. R., Brooks, B., Drake, N., Jickells, T. D., and Benning, L. G.: Minor effect of physical size sorting on iron solubility of transported mineral dust, Atmos. Chem. Phys., 11, 8459-8469, https://doi.org/10.5194/acp-11-8459-2011, 2011.
- Sholkovitz, E. R., Sedwick, P. N., and Church, T. M.: Influence of anthropogenic combustion emissions on the deposition of soluble aerosol iron to the ocean: Empirical estimates for island sites in the North Atlantic, Geochim. Cosmochim. Acta, 73, 3981-4003, https://doi.org/10.1016/j.gca.2009.04.029, 2009.
- Song, M., Jeong, R., Kim, D., Qiu, Y., Meng, X., Wu, Z., Zuend, A., Ha, Y., Kim, C., Kim, H., Gaikwad, S., Jang, K. S., Lee, J. Y., and Ahn, J.: Comparison of Phase States of PM(2.5) over Megacities, Seoul and Beijing, and Their Implications on Particle Size Distribution, Environ. Sci. Technol., 56, 17581-17590, https://doi.org/10.1021/acs.est.2c06377, 2022.
- Sullivan, R. C., Guazzotti, S. A., Sodeman, D. A., and Prather, K. A.: Direct observations of the atmospheric processing of Asian mineral dust, Atmos. Chem. Phys., 7, 1213-1236, https://doi.org/10.5194/acp-7-1213-2007, 2007.
- Sun, J., Liu, L., Xu, L., Wang, Y., Wu, Z., Hu, M., Shi, Z., Li, Y., Zhang, X., Chen, J., and Li, W.: Key Role of
 Nitrate in Phase Transitions of Urban Particles: Implications of Important Reactive Surfaces for
 Secondary Aerosol Formation, J. Geophys. Res.-Atmos., 123, 1234-1243,
 https://doi.org/10.1002/2017JD027264, 2018.
- Takahashi, Y., Higashi, M., Furukawa, T., and Mitsunobu, S.: Change of iron species and iron solubility in Asian
 dust during the long-range transport from western China to Japan, Atmos. Chem. Phys., 11, 11237 11252, https://doi.org/10.5194/acp-11-11237-2011, 2011.
- 747 Tang, M., Cziczo, D. J., and Grassian, V. H.: Interactions of Water with Mineral Dust Aerosol: Water

- 748 Adsorption, Hygroscopicity, Cloud Condensation, and Ice Nucleation, Chem. Rev., 116, 4205-4259, 749 https://doi.org/10.1021/acs.chemrev.5b00529, 2016.
- 750 Taylor, S. R., and McLennan, S. M.: The continental crust: Its composition and evolution, Blackwell Scientific 751 Publications, Oxford, 312 pp., 1985.
- 752 Trochkine, D., Iwasaka, Y., Matsuki, A., Yamada, M., Kim, Y.-S., Nagatani, T., Zhang, D., Shi, G.-Y., and Shen, 753 Z.: Mineral aerosol particles collected in Dunhuang, China, and their comparison with chemically 754 modified particles collected over Japan, J. Geophys. Res.-Atmos., 108, 8642, 755 https://doi.org/10.1029/2002JD003268, 2003.
- 756 Virkkula, A., Teinilä, K., Hillamo, R., Kerminen, V. M., Saarikoski, S., Aurela, M., Viidanoja, J., Paatero, J., 757 Koponen, I. K., and Kulmala, M.: Chemical composition of boundary layer aerosol over the Atlantic 758 Ocean and at an Antarctic site, Atmos. Chem. Phys., 6, 3407-3421, https://doi.org/10.5194/acp-6-3407-759 **2006**, 2006.
- 760 Walters, W. W., and Hastings, M. G.: Collection of Ammonia for High Time-Resolved Nitrogen Isotopic 761 Characterization Utilizing an Acid-Coated Honeycomb Denuder, Anal. Chem., 90, 8051-8057, 762 https://doi.org/10.1021/acs.analchem.8b01007, 2018.

765

767

768

769

770

- 763 Wang, G. H., Cheng, C. L., Huang, Y., Tao, J., Ren, Y. O., Wu, F., Meng, J. J., Li, J. J., Cheng, Y. T., Cao, J. J., Liu, S. X., Zhang, T., Zhang, R., and Chen, Y. B.: Evolution of aerosol chemistry in Xi'an, inland China, during the dust storm period of 2013 - Part 1: Sources, chemical forms and formation 766 mechanisms of nitrate and sulfate, Atmos. Chem. Phys., 14, 11571-11585, https://doi.org/10.5194/acp-14-11571-2014, 2014.
 - Wang, S., Yan, Q., Zhang, R., Jiang, N., Yin, S., and Ye, H.: Size-fractionated particulate elements in an inland city of China: Deposition flux in human respiratory, health risks, source apportionment, and dry deposition, Environmental Pollution, 247, 515-523, https://doi.org/10.1016/j.envpol.2019.01.051,
- 772 Westberry, T. K., Behrenfeld, M. J., Shi, Y. R., Yu, H., Remer, L. A., and Bian, H.: Atmospheric nourishment of 773 global ocean ecosystems, Science, 380, 515-519, https://doi.org/10.1126/science.abq5252, 2023.
- 774 Wu, F., Zhang, D., Cao, J., Guo, X., Xia, Y., Zhang, T., Lu, H., and Cheng, Y.: Limited production of sulfate and 775 nitrate on front-associated dust storm particles moving from desert to distant populated areas in 776 northwestern China, Atmos. Chem. Phys., 17, 14473-14484, https://doi.org/10.5194/acp-17-14473-777 2017, 2017.
- 778 Wuttig, K., Wagener, T., Bressac, M., Dammshäuser, A., Streu, P., Guieu, C., and Croot, P. L.: Impacts of dust 779 deposition on dissolved trace metal concentrations (Mn, Al and Fe) during a mesocosm experiment, 780 Biogeosciences, 10, 2583-2600, 10.5194/bg-10-2583-2013, 2013.
- 781 Xu, H., and Weber, T.: Ocean Dust Deposition Rates Constrained in a Data-Assimilation Model of the Marine 782 Aluminum Cycle, Global Biogeochem. Cycles, 35, e2021GB007049, 783 https://doi.org/10.1029/2021GB007049, 2021.
- 784 Yang, J., Ma, L., He, X., Au, W. C., Miao, Y., Wang, W. X., and Nah, T.: Measurement report: Abundance and 785 fractional solubilities of aerosol metals in urban Hong Kong - insights into factors that control aerosol 786 metal dissolution in an urban site in South China, Atmos. Chem. Phys., 23, 1403-1419, 787 https://doi.org/10.5194/acp-23-1403-2023, 2023.
- 788 Zhang, H., Li, R., Dong, S., Wang, F., Zhu, Y., Meng, H., Huang, C., Ren, Y., Wang, X., Hu, X., Li, T., Peng, C., 789 Zhang, G., Xue, L., Wang, X., and Tang, M.: Abundance and Fractional Solubility of Aerosol Iron 790 During Winter at a Coastal City in Northern China: Similarities and Contrasts Between Fine and

791 Coarse Particles, J. Geophys. Res.-Atmos., 127, e2021JD036070, 792 https://doi.org/10.1029/2021JD036070, 2022. 793 Zhang, H., Li, R., Huang, C., Li, X., Dong, S., Wang, F., Li, T., Chen, Y., Zhang, G., Ren, Y., Chen, Q., Huang, 794 R., Chen, S., Xue, T., Wang, X., and Tang, M.: Seasonal variation of aerosol iron solubility in coarse 795 and fine particles at an inland city in northwestern China, Atmos. Chem. Phys., 23, 3543-3559, 796 https://doi.org/10.5194/acp-23-3543-2023, 2023. 797 Zhang, L., Kojima, T., and Zhang, D.: Origins and Aging of Calcium-rich Mineral Particles in Asian Dust 798 Arriving in Southwestern Japan: A Comparison of Slow- and Fast-moving Events, Aerosol Sci. Eng., 799 https://doi.org/10.1007/s41810-024-00275-z, 2024. 800 Zhang, R., Jing, J., Tao, J., Hsu, S. C., Wang, G., Cao, J., Lee, C. S. L., Zhu, L., Chen, Z., Zhao, Y., and Shen, 801 Z.: Chemical characterization and source apportionment of PM_{2.5} in Beijing: seasonal perspective, 802 Atmos. Chem. Phys., 13, 7053-7074, https://doi.org/10.5194/acp-13-7053-2013, 2013. 803 Zhang, X. Y., Gong, S. L., Shen, Z. X., Mei, F. M., Xi, X. X., Liu, L. C., Zhou, Z. J., Wang, D., Wang, Y. Q., and 804 Cheng, Y.: Characterization of soil dust aerosol in China and its transport and distribution during 2001 805 ACE-Asia: 1. Network observations, J. Geophys. Res.-Atmos., 108, 4261, 806 https://doi.org/10.1029/2002JD002632, 2003. 807 Zhi, M., Wang, G., Xu, L., Li, K., Nie, W., Niu, H., Shao, L., Liu, Z., Yi, Z., Wang, Y., Shi, Z., Ito, A., Zhai, S., 808 and Li, W.: How Acid Iron Dissolution in Aged Dust Particles Responds to the Buffering Capacity of 809 Carbonate Minerals during Asian Dust Storms, Environ. Sci. Technol., 59, 6167-6178,

https://doi.org/10.1021/acs.est.4c12370, 2025.

810

Text S1. Sampling sites

1

At Xi'an, sampling in spring, summer and autumn was conducted on a building roof 2 (~40 m above the ground level) at Shaanxi University of Science and Technology (34°22'N, 3 108°58'E). This site is surrounded by residential areas, with no major industrial sources nearby. 4 Sampling in winter was carried out on a building roof (~10 m above the ground level) at the 5 6 Institute of Earth Environment, Chinese Academy of Sciences (34°13'N, 108°53'E). This site 7 is surrounded by commercial and residential areas. Both sampling sites are urban sites (Zhang et al., 2023). 8 9 At Qingdao, sampling was conducted on the rooftop of a 5-floor building in northeastern Qingdao (36°20'N, 120°39'E). This rural/suburban site, which is ~28 m above the ground level 10 and ~1.3 km from the coastline, is surrounded by some residence and office buildings, villages 11 12 and agricultural fields (Zhang et al., 2022). 13 14

Table S1. Brief summary of atmospheric sampling at Xi'an and Qingdao.

Location	Season	Sample period	Number of samples
	spring	01 to 30 April 2021	28
Xi'an	summer	12 July to 14 August 2021	32
Al an	autumn	07 October to 06 November	30
	winter	01 November to 30 December 2020	36
	spring	20 March to 22 April 2023	28
Oin a da a	summer	20 June to 26 July 2022	26
Qingdao	autumn	04 to 31 October 2022	27
	winter	23 November to 24 December 2022	25

Table S2. Summary of total aerosol Al concentrations (μg/m³) measured over East Asian and the Pacific Ocean.

Location	Geographic coordinates	Sampling period	Size range	Average	Range	reference
Aksu, China	40°16'N, 80°28'E	May to June 2001	TSP	24	/	Zhang et al. (2003)
Urumqi, China	43°49'N, 87°37'E	January 2004 to March 2007	TSP	8.05	/	Li et al. (2008)
Wuhai, China	39°39'N, 106°49'E	March 2021	PM _{2.5}	7.77±19.15	0.00-195.79	Meng et al. (2023)
Xi'an, China	34°22'N, 108°58'E	November 2020 to November	$d_p > 1 \mu m$	1.42±0.86	0.16-3.70	This study
		2021	$d_p < 1 \mu m$	2.28±2.35	0.14-14.88	
Yulin, China	38°17'N, 109°28'E	Spring 2006-2008	TSP	36.38 (dust)	/	Wang et al. (2011)
				6.91 (non-dust)	/	
Beijing, China	39°97' N, 116°21'E	March to May 2012	PM _{2.5}	3.97±1.26 (dust)	/	Liu and Bei (2016)
				0.76±0.61 (non-dust)	/	
Jinan, China	36°40'N, 117°09'E	March 2021	PM _{2.5}	1.10±2.56	0.00-20.68	Meng et al. (2023)
Qingdao, China	36°20'N, 120°39'E	November 2022 to March 2023	$d_p > 1 \mu m$	0.56±0.75	0.08-4.01	This study
			$d_p < 1 \mu m$	1.08 ± 1.67	0.05-9.63	
Huaniao Island, China	30°51'N, 122°40'E	April 2010 to March 2011	TSP	/	0.075-16	Guo et al. (2014)
Higashi-Hiroshima,	34°24'N, 132°42'E	December 2012 to December	TSP	/	0.17-1.716	Sakata et al.
Japan		2013				(2023)
The Pacific Ocean	21°15′N, 157°45′W	January and June 2002	TSP	/	0.001-0.056	Measures et al.
(Hawaii)						(2010)
The Pacific Ocean	along 30°N	June to August 2004	TSP	0.078	0.012-0.475	Buck et al. (2013)

Table S3. Overview of total aerosol Al concentrations ($\mu g/m^3$) for submicron and supermicron

22 particles at Xi'an and Qingdao.

Location	C.	subm	icron particle	es	supermicron particles		
	Season	range	mean	median	range	mean	median
	spring	0.14-14.88	4.29±3.70	3.32	0.25-3.70	1.54±0.89	1.59
V :2	summer	0.17-2.01	0.95±0.44	0.90	0.16-1.96	0.96±0.54	0.97
Xi'an	autumn	0.20-2.26	1.06±0.48	1.03	0.22-2.75	1.22±0.72	1.07
	winter	0.32-6.11	2.92±1.47	3.02	0.31-3.53	1.91±0.93	1.91
	spring	0.18-9.63	1.88±2.51	0.93	0.29-3.69	1.04±1.12	0.48
0' 1	summer	0.05-0.85	0.35±0.22	0.35	0.08-0.63	0.33±0.18	0.37
Qingdao	autumn	0.27-1.32	0.65±0.22	0.63	0.13-0.57	0.31±0.12	0.30
	winter	0.40-9.17	1.40±1.82	0.81	0.12-4.01	0.51±0.77	0.29

Table S4. Overview of dissolved aerosol Al concentrations (ng/m³) for submicron and supermicron particles at Xi'an and Qingdao.

Location	C	subm	nicron particle	es	supermicron particles		
	Season	range	mean	median	range	mean	median
	spring	0.3-359.4	65.4±79.2	40.1	1.2-47.2	23.1±10.9	24.8
V :?	summer	3.3-100.9	23.2±23.4	17.3	3.6-37.2	15.0±8.7	13.1
Xi'an	autumn	6.0-120.2	22.6±20.1	19.3	1.2-37.0	13.2±8.6	12.5
	winter	3.1-97.3	25.6±19.8	22.1	9.2-43.7	19.6±8.2	17.5
	spring	2.5-20.9	8.7±5.8	6.2	1.1-41.3	8.8±10.8	5.3
0' 1	summer	0.4-30.6	10.2±8.2	8.9	1.3-40.2	12.8±11.1	9.4
Qingdao	autumn	1.3-23.0	6.0±4.8	5.2	0.3-49.0	7.9±10.5	3.5
	winter	1.8-63.3	14.5±15.2	9.4	1.4-54.9	12.8±12.9	8.9

Table S5. Overview of aerosol Al solubility (%) for submicron and supermicron particles at

30 Xi'an and Qingdao.

Location	C	subm	nicron particle	es	supermicron particles		
	Season	range	mean	median	range	mean	median
	spring	0.11-7.74	1.46±1.48	1.01	0.45-4.84	1.75±1.04	1.38
Xi'an	summer	0.74-9.10	2.40±2.03	1.69	0.76-4.71	1.83±0.95	1.59
Al all	autumn	1.21-7.36	2.23±1.40	1.82	0.25-2.64	1.17±0.54	1.04
	winter	0.31-3.55	0.99±0.75	0.74	0.43-7.70	1.42±1.47	1.01
	spring	0.14-4.23	0.93±1.02	0.61	0.06-8.91	1.58±2.29	0.54
O: 4	summer	0.11-11.11	3.27±2.55	2.33	0.69-12.79	4.55±3.61	3.56
Qingdao	autumn	0.18-3.44	1.01±0.86	0.69	0.18-14.77	2.74±3.56	1.17
	winter	0.32-5.03	1.26±1.05	0.93	0.30-23.35	4.21±5.35	2.39

Table S6. Overview of total Al (μ g/m³), dissolved Al (ng/m³) and Al solubility (%) under different weather conditions for submicron and supermicron particles at Xi'an.

	subi	micron particles	super	rmicron particle	es	
total Al	range	average	median	range	average	median
entire	0.14-14.88	2.28±2.35	1.40	0.16-3.70	1.42±0.86	1.31
clean	0.28-6.73	1.67±1.39	1.30	0.16-2.49	1.07±0.58	1.13
dust	2.75-14.88	8.54±4.24	8.40	0.92-3.70	2.25±1.06	2.22
haze	0.32-5.94	2.59±1.32	2.21	0.31-3.53	2.08±0.91	2.23
dissolved Al	range	average	median	range	average	median
entire	0.3-359.4	33.1±44. 7	20.4	1.15-47.3	17.7±9.7	16.3
clean	0.3-125.8	28.1±25.3	21. 7	1.21-37.2	14.6±8.3	13.4
dust	54.1-359.4	146.1±109.6	139.1	24.8-47.2	34.5±8.7	34.3
haze	7.6-80.8	20.0±21.1	15.0	11.3-43.7	22.2±9.3	21.2
Al solubility	range	average	median	range	average	median
entire	0.11-9.10	1.75±1.57	1.32	0.25-7.70	1.54±1.10	1.22
clean	0.11-9.10	1.96±1.62	1.64	0.25-4.71	1.51±0.75	1.29
dust	0.42-7.74	2.31±2.49	1.86	0.77-4.84	2.08±1.55	1.47
haze	0.31-3.22	0.96±0.71	0.72	0.43-7.70	1.49±1.71	1.01

Table S7. Overview of total Al (μg/m³), dissolved Al (ng/m³) and Al solubility (%) under
 different weather conditions for submicron and supermicron particles at Qingdao.

	submicron particles				supermicron particles			
total Al	range	average	median	range	average	median		
entire	0.05-9.63	1.08±1.67	0.68	0.08-4.01	0.56±0.75	0.36		
clean	0.08-1.34	0.66±0.28	0.68	0.08-1.15	0.31±0.17	0.30		
dust	1.05-9.63	6.42±3.08	7.14	0.66-4.01	2.90±1.10	2.96		
haze	0.77-1.90	1.40±0.58	1.55	0.47-1.09	0.69±0.35	0.50		
fog	0.18-1.09	0.53±0.35	0.42	0.17-0.52	0.38±0.14	0.37		
dissolved Al	range	average	median	range	average	median		
entire	0.4-63.3	9.8±9.6	6.1	0.3-54.9	10.5±11.4	6.3		
clean	0.4-40.6	6.2±5.7	5.4	0.9-26.6	5.1±5.0	3.0		
dust	2.5-63.3	25. 9±20.9	20.6	1.9-23.6	11.5±7.5	10.4		
haze	24.5-26.6	25.4±1.1	25.2	14.2-39.7	23.7±14.0	17.3		
fog	4.0-19.5	7.4±5.5	5.2	8.7-54.6	29.4±17.2	34.8		
Al solubility	range	average	median	range	average	median		
entire	0.11-11.11	1.60±1.78	0.91	0.06-23.35	3.23±3.95	1.70		
clean	0.11-8.30	1.15±1.26	0.77	0.18-15.58	2.10±2.72	0.99		
dust	0.20-1.50	0.45±0.47	0.24	0.06-2.87	0.67±0.98	0.31		
haze	1.40-3.27	2.09±1.03	1.58	2.85-3.70	3.40±0.47	3.64		
fog	0.43-4.23	1.93 ±1.52	1.38	2.37-23.35	9.09±7.26	6.90		

- Table S8. Pearson correlations coefficient (*r*): aerosol Al solubility versus [sulfate]/[Al] and [nitrate]/[Al] for submicron and supermicron particles at Xi'an and Qingdao. In this table, *r*
- values which are >0.5 are highlighted in bold.

		Xi	a'an	Qin	Qingdao		
Species	Season	submicron particles	supermicron particles	submicron particles	supermicron particles		
	spring	-0.33	0.33	0.87	0.75		
[sulfate]/[Al]	summer	-0.17	0.36	0.68	0.66		
	autumn	0.15	0.58	0.59	0.84		
	winter	0.57	0.73	0.17	0.96		
[nitrate]/[Al]	spring	-0.37	0.25	0.89	0.71		
	summer	-0.20	0.29	0.14	0.59		
	autumn	-0.12	0.70 (0.41*)	0.70	0.90		
	winter	0.32	0.93 (0.44*)	0.30	0.88		

^{*} Pearson correlations coefficients (r) after three outliers for which aerosol Al solubility was

44

very high were excluded.

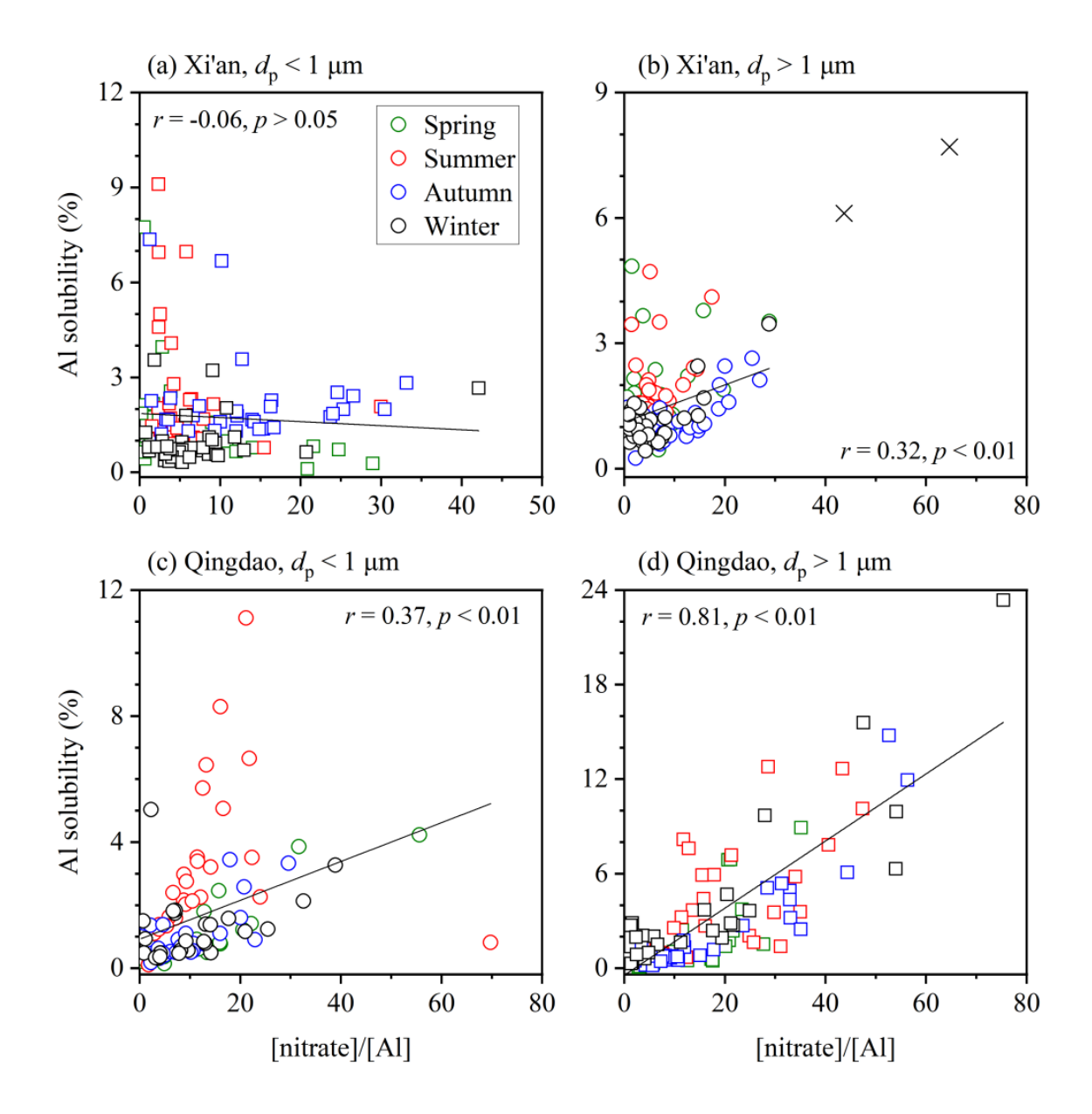


Figure S1. Aerosol Al solubility versus [nitrate]/[Al]: (a) submicron particles at Xi'an; (b) supermicron particles at Xi'an; (c) submicron particles at Qingdao; (d) supermicron particles at Qingdao. Data represented by crosses are not included in fittings.

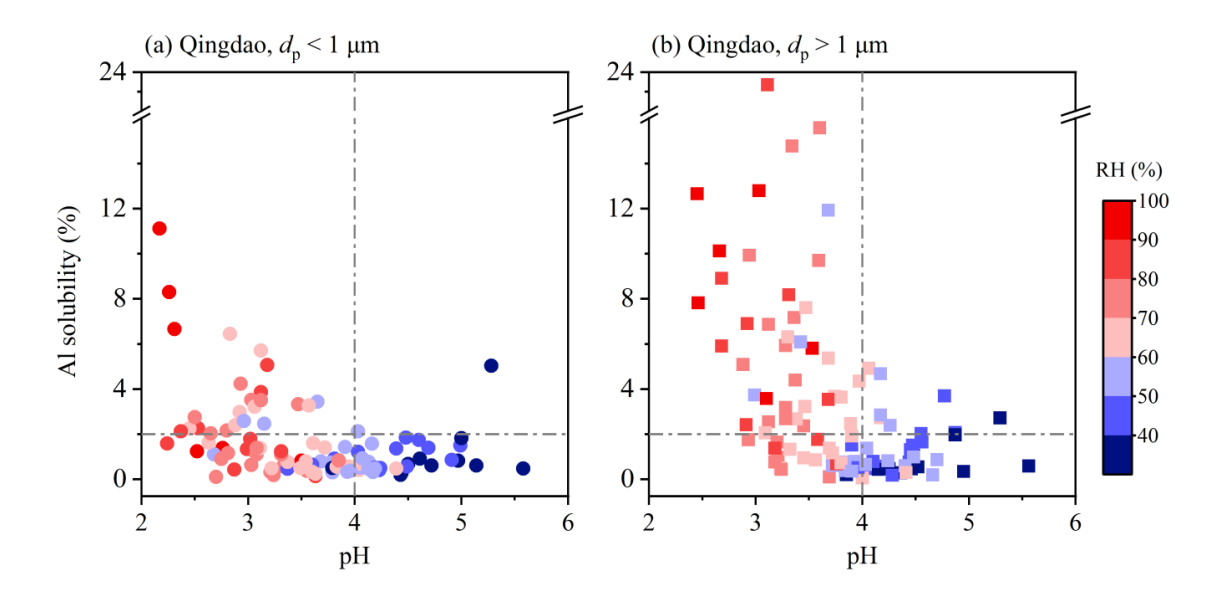


Figure S2. Dependence of aerosol Al solubility on relative humidity (RH) and aerosol pH at Qingdao: (a) submicron particles; (b) supermicron particles.

References

57

70 71

72

73

78 79

80

- Buck, C. S., Landing, W. M., and Resing, J.: Pacific Ocean aerosols: Deposition and solubility of iron, aluminum, and other trace elements, Mar. Chem., 157, 117-130, https://doi.org/10.1016/j.marchem.2013.09.005, 2013.
- Guo, L., Chen, Y., Wang, F., Meng, X., Xu, Z., and Zhuang, G.: Effects of Asian dust on the atmospheric input of trace elements to the East China Sea, Mar. Chem., 163, 19-27, https://doi.org/10.1016/j.marchem.2014.04.003, 2014.
- Li, J., Zhuang, G., Huang, K., Lin, Y., Xu, C., and Yu, S.: Characteristics and sources of airborne particulate in Urumqi, China, the upstream area of Asia dust, Atmos. Environ., 42, 776-787, https://doi.org/10.1016/j.atmosenv.2007.09.062, 2008.
- Liu, Q., and Bei, Y.: Impacts of crystal metal on secondary aliphatic amine aerosol formation during dust storm episodes in Beijing, Atmos. Environ., 128, 227-234, https://doi.org/10.1016/j.atmosenv.2016.01.013, 2016.
 - Measures, C. I., Sato, T., Vink, S., Howell, S., and Li, Y. H.: The fractional solubility of aluminium from mineral aerosols collected in Hawaii and implications for atmospheric deposition of biogeochemically important trace elements, Mar. Chem., 120, 144-153, https://doi.org/10.1016/j.marchem.2009.01.014, 2010.
- Meng, Q., Yan, C., Li, R., Zhang, T., Zheng, M., Liu, Y., Zhang, M., Wang, G., Du, Y., Shang, C., and Fu, P.: Variations of PM2.5-bound elements and their associated effects during long-distance transport of dust storms: Insights from multi-sites observations, Sci. Total Environ., 889, 164062, https://doi.org/10.1016/j.scitotenv.2023.164062, 2023.
 - Sakata, K., Sakaguchi, A., Yamakawa, Y., Miyamoto, C., Kurisu, M., and Takahashi, Y.: Measurement report: Stoichiometry of dissolved iron and aluminum as an indicator of the factors controlling the fractional solubility of aerosol iron results of the annual observations of size-fractionated aerosol particles in Japan, Atmos. Chem. Phys., 23, 9815-9836, https://doi.org/10.5194/acp-23-9815-2023, 2023.
- Wang, Q., Zhuang, G., Li, J., Huang, K., Zhang, R., Jiang, Y., Lin, Y., and Fu, J. S.: Mixing of dust with pollution on the transport path of Asian dust Revealed from the aerosol over Yulin, the north edge of Loess Plateau, Sci. Total Environ., 409, 573-581, https://doi.org/10.1016/j.scitotenv.2010.10.032, 2011.
- Zhang, H., Li, R., Dong, S., Wang, F., Zhu, Y., Meng, H., Huang, C., Ren, Y., Wang, X., Hu, X., Li, T., Peng, C., Zhang, G., Xue, L., Wang, X., and Tang, M.: Abundance and Fractional Solubility of Aerosol Iron During Winter at a Coastal City in Northern China: Similarities and Contrasts Between Fine and Coarse Particles, J. Geophys. Res.-Atmos., 127, e2021JD036070, https://doi.org/10.1029/2021JD036070, 2022.
- Zhang, H., Li, R., Huang, C., Li, X., Dong, S., Wang, F., Li, T., Chen, Y., Zhang, G., Ren, Y., Chen, Q., Huang, R., Chen, S., Xue, T., Wang, X., and Tang, M.: Seasonal variation of aerosol iron solubility in coarse and fine particles at an inland city in northwestern China, Atmos. Chem. Phys., 23, 3543-3559, https://doi.org/10.5194/acp-23-3543-2023, 2023.
- Zhang, X. Y., Gong, S. L., Shen, Z. X., Mei, F. M., Xi, X. X., Liu, L. C., Zhou, Z. J., Wang, D.,
 Wang, Y. Q., and Cheng, Y.: Characterization of soil dust aerosol in China and its
 transport and distribution during 2001 ACE-Asia: 1. Network observations, J. Geophys.

100 Res.-Atmos., 108, 4261, https://doi.org/10.1029/2002JD002632, 2003.